The University of Alberta
Printing Department
Edmonton, Alberta

THE UNIVERSITY OF ALBERTA

LOCAL BUCKLING OF COMPOSITE BEAMS IN NEGATIVE BENDING

BY

© JOHN HANSEN

A THESIS

SUBMITTED TO THE FACULTY OF GRADUATE STUDIES

IN PARTIAL FULFILLMENT OF THE REQUIREMENTS FOR THE DEGREE OF

MASTER OF SCIENCE

DEPARTMENT OF CIVIL ENGINEERING

EDMONTON, ALBERTA

SPRING, 1971

UNIVERSITY OF ALBERTA

FACULTY OF GRADUATE STUDIES

The undersigned certify that they have read, and recommend to the Faculty of Graduate Studies for acceptance, a thesis entitled "LOCAL BUCKLING OF COMPOSITE BEAMS IN NEGATIVE BENDING" submitted by John Hansen in partial fulfillment for the degree of Master of Science.

ABSTRACT

A theoretical behavioural study of composite beams in negative bending is presented, with emphasis on the effect of longitudinal slab reinforcement. A method for determining the moment producing local buckling of the compression flange is developed and a computer program for the plotting of the moment - curvature and related relationships is presented. Analytical results are compared with the results of tests previously conducted at the University of Alberta.

Two approaches are used in obtaining the flexural behaviour relationships; one based on an idealized stress-strain diagram consisting of elastic, plastic and strain-hardening regions, the other based on a modified stress-strain diagram consisting of elastic and strain-hardening regions. Restraint afforded the flange by the web is based on the location of the neutral axis. An upper limit is placed on the effectiveness of the longitudinal slab reinforcement.

The analysis based on the modified stress-strain diagram, in which the two regions are defined by an elastic modulus, E, and a strain-hardening modulus, E'_{st}, provides a satisfactory method for determining the moment at local buckling for composite beams in which strain-hardening strains are reached in the compression flange. Although there is a considerable

variation between theoretical and experimental values of curvature at ultimate moment, it is considered unlikely that any theoretical analysis will provide any better agreement.

ACKNOWLEDGEMENTS

The author wishes to express his sincere appreciation to the following for their contribution to this thesis.

The investigation was made possible through financial assistance provided by the National Research Council of Canada.

Professor J. Longworth supervised the investigation and his assistance throughout the program was invaluable.

Mrs. M. J. Hansen typed the manuscript.

TABLE OF CONTENTS

LIST OF TABLES

LIST OF FIGURES

LIST OF NOTATION

A_f	Area of flange
A_s	Area of longitudinal slab reinforcement
A'_s	Upper limit on area of slab reinforcement
A_w	Area of web
A_{WF}	Area of steel section
D_x, D_y	Plate stiffness coefficients - direct stiffness
D_{xy}, D_{yx}	Plate stiffness coefficients - cross stiffness
E	Modulus of elasticity
E_{st}	Strain-hardening modulus, idealized stress-strain diagram
E'_{st}	Strain-hardening modulus, modified stress-strain diagram
E_t	Tangent modulus
E_x, E_y	Tangent modulus in x and y direction
F_{cr}	Critical stress
F_y	Yield stress
F_{ys}	Yield stress of slab reinforcement
F_u	Ultimate stress
G_e	Elastic shear modulus
G_t	Inelastic shear Modulus
H	$D_{xy} + D_{yx} + 4G_t$
I	Moment of inertia
I_ω	Warping moment of inertia
K_t	Uniform torsion constant
L	Length of plate
M_o	Moment at first yield of compression flange
M_p	Simple plastic moment

M_p^o	Simple plastic moment of steel beam
M_x, M_y	Bending moments in x and y direction
M_{xy}	Twisting moment
M_{ult}	Ultimate moment
M_{ult}^o	Ultimate moment of steel section
P	Load
P_{ult}	Ultimate load
a	Length of plate
b	Half-flange width
¢	Centreline
c_1, c_2, c_3, c_4, c_5, c_6, c_7	Constants of integration
d	Depth of steel section
f_x	Edge compression stress in x direction
h	Depth of web
h'	E/E_{st}
k	Plate buckling coefficient
k_s	Torsional spring constant
ℓ	Critical length
ℓ_b	Half-wavelength of local buckle
m, n	Number of half-waves into which plate buckles in x and y direction
w	Thickness of web

z	Distance to neutral axis from compression web-flange junction
β	Degree of restraint of plate edges
$\delta_{\text{¢}}$	Centreline deflection
δ_{ult}	Deflection at ultimate moment
ε_y	Yield strain
ε_{st}	Strain-hardening strain
γ	E_t/E
θ_{total}	Total rotation
θ_{ult}	Rotation at ultimate moment
ϕ	Curvature
ϕ_o	Curvature at first yield of compression flange
ϕ_{ult}	Curvature at ultimate moment
τ_L	Yielded length of flange
μ	Poisson's ratio
μ_x, μ_y	Poisson's ratio in x and y direction
ω, $\omega(x,y)$	Deflected shape of plate

CHAPTER I

INTRODUCTION

1.1 INTRODUCTORY REMARKS

In order to realize the full advantage of composite construction applied to flexural members it is necessary to develop continuity. The behaviour of composite beams in resisting positive moment is well defined; however, the behaviour of composite beams under negative moment is not as fully understood. In negative moment regions longitudinal slab reinforcement may be introduced to increase the moment capacity since the concrete slab is ineffective in tension. Test results indicate that this reinforcement effectively increases the negative moment resistance and current design specifications permit full contribution of longitudinal reinforcement.

In the design of structural steel flexural members, care is taken to prevent premature local buckling of the compression elements. Local buckling must also be considered in composite beams, particularly in continuous spans. Conditions in positive moment regions present little problem as the presence of the concrete slab in the compression zone tends to reduce the depth of the steel section in compression, thereby reducing the probability of local buckling. Furthermore, the slab tends to stiffen the compression flange. In negative bending, however, the concrete slab is connected to the tension flange of the steel section. If longitudinal reinforcement is present, most of the

steel section is in compression. Also, in negative bending, the compression flange is remote from the slab. Therefore, local buckling is more significant in negative moment regions.

Recent experimental investigations have provided information concerning the buckling behaviour of composite beams in negative bending.

1.2 RESEARCH AT THE UNIVERSITY OF CAMBRIDGE

Tests simulating the negative moment region of a continuous beam were carried out by van Dalen in 1966 on simple span composite beams. The modes of failure observed included crushing of the bottom surface of the concrete slab, longitudinal splitting of the slab, shear failure in the slab, buckling of the compression flange and buckling of the web of the steel section.

Results of this investigation indicated that the resistance to bending in a negative moment region, with longitudinal slab reinforcement present, continues to increase with curvature until buckling occurs in the steel section. This was true provided adequate shear connection and transverse slab reinforcement were provided. Cracking of the concrete slab, due to tensile forces present, did not affect this behaviour. It was concluded that, using the assumption of complete interaction and plane sections, reliable predictions of the observed longitudinal strains, curvature and rotations, at all loads up to the ultimate load, may be obtained.

1.3 RESEARCH AT THE UNIVERSITY OF ALBERTA

Three experimental investigations have been conducted in the Department of Civil Engineering at the University of Alberta concerning

the behaviour of composite beams in negative bending. The beams tested consisted of rolled steel sections connected by headed stud shear connectors to reinforced cast-in-place concrete slabs.

In 1968 Piepgrass (1) tested six specimens representing an isolated negative moment region. The main variables were slab width and the amount of longitudinal slab reinforcement. Four of the six beams were coverplated. One of the remaining beams was coverplated after the initial test and retested. The failure mode of the beams without coverplates was local buckling of the flange and web. The beams with coverplates failed by lateral buckling. It was concluded that the ultimate capacity of the composite section increased as the longitudinal slab reinforcement was increased. It was also indicated that a steel section defined a compact section under the provisions of current specifications had significantly reduced rotation capacity in a composite section as compared with that of the plane beam. This reduced rotation capacity might be of concern in plastic design in relation to the effect on the development of a mechanism.

Davison (2) in 1969 studied the effect of longitudinal slab reinforcement on the rotation capacity of composite sections in negative bending. Seven beams with varying slab widths were tested. Failure of the beams occurred by local buckling of the web, local buckling of the compression flange or a combination of the two.

The addition of longitudinal slab reinforcement was found to significantly increase the ultimate negative moment capacity. The increase, however, was not proportional to the increase in simple plastic moment values. As the longitudinal slab reinforcement increased, the

rotation capacity decreased. The width of the concrete slab had no significant effect on the ultimate moment capacity or rotation capacity. The longitudinal slab reinforcement reached yield prior to the attainment of ultimate moment.

In a third study by Lever (3) in 1970, nine beams were tested in negative bending. The main objective was to study the effect of varying the size of the steel section and to further study the effects of varying the amount of longitudinal slab reinforcement. The beams failed by local buckling of the compression flange and web, either separately or in combination.

The major conclusions drawn from the three investigations carried out at the University of Alberta are as follows:

1. The addition of longitudinal slab reinforcement can result in significant increases in the ultimate moment capacity of composite beams in negative bending.
2. The increase in ultimate moment is not directly proportional to the increase in the theoretical plastic moment.
3. For a given steel section, a reduction in the rotation capacity of a negative plastic hinge occurs with an increase in the amount of longitudinal slab reinforcement.
4. Slip between the concrete slab and steel section increases with load. The slip becomes concentrated in the region of the beam nearest to the local buckle after buckling has occurred.

5. Slip between the concrete slab and the steel section significantly affects the strains in the longitudinal reinforcement. In all tests, strains at ultimate load reached the yield strain, but were considerably less than the value determined by extending the strain profiles from the steel section to the level of longitudinal reinforcement.

6. Cracking behaviour of the concrete slab is influenced by the amount of longitudinal slab reinforcement, the spacing of the transverse reinforcement, and the transverse curvature of the slab. A few wide cracks develop for low amounts of reinforcement. Increasing the amount of slab reinforcement results in an increase in the number of cracks and a decrease in the crack width.

1.4 SCOPE OF THE PRESENT INVESTIGATION

The primary objectives of the present investigation are to obtain theoretical values for local buckling moments and to develop theoretical moment-curvature relationships for composite beams in negative bending.

CHAPTER II

LOCAL BUCKLING OF STEEL BEAMS

2.1 PLATE BUCKLING IN THE ELASTIC RANGE

Local buckling of the compression flange of an "I" section, due to axial load or bending, is essentially the buckling of a plate subjected to uniformly distributed compressive stresses. The correct differential equation of a buckled plate was first developed by Navier in 1823. The solution of this differential equation is credited to Bryan in 1888. For a simply supported rectangular plate with edge compression in one direction, the differential equation has the form

$$\frac{Et^3}{12(1-\mu^2)}\left(\frac{\partial^4\omega}{\partial x^4}+\frac{2\partial^4\omega}{\partial x^2\partial y^2}+\frac{\partial^4\omega}{\partial y^4}\right)=-f_x\ t\frac{\partial^2\omega}{\partial x^2} \qquad (2\text{-}1)$$

where f_x is the edge compression stress as shown in FIGURE 2-1. The deflected shape may be assumed in the form of a series, each term of which satisfies the boundary conditions.

$$\omega=\omega(x,y)=\sum_{m=1,2,3}^{\infty}\sum_{n=1,2,3}^{\infty}A_{mn}\sin\frac{m\pi x}{a}\sin\frac{n\pi y}{b} \qquad (2\text{-}2)$$

From EQUATIONS (2-1) and (2-2) the critical stress is found to be

$$F_{cr}=f_x=\frac{\pi^2E}{12(1-\mu^2)}\left(\frac{t}{b}\right)^2\left(m\frac{b}{a}+\frac{a}{b}\frac{n^2}{m}\right)^2 \qquad (2\text{-}3)$$

in which the quantities m and n represent the number of half-waves into which the plate buckles in the x and y directions. The term $\left(m\frac{b}{a}+\frac{a}{b}\frac{n^2}{m}\right)^2$ is defined as the plate buckling coefficient "k". Regardless of the boundary conditions, the critical stress for any

rectangular plate subjected to edge compression in one direction may be expressed as

$$F_{cr} = k\pi^2 \frac{E}{12(1-\mu^2)}\left(\frac{t}{b}\right)^2 \qquad (2\text{-}4)$$

in which k, the plate buckling coefficient depends on the boundary conditions.

For a comparatively long steel plate, with boundary conditions representative of the flange of an "I" section (y = 0 fixed and y = b free) the value of k is 1.328 and

$$F_{cr} = 3600\ t^2/b^2$$

from which

$$(b/t)_{cr} = 190/\sqrt{F_{cr}} \qquad (2\text{-}5)$$

where b equals half the total flange width. Since the buckling is elastic, F_{cr} is limited to the yield stress of the material, F_y. EQUATION (2-5) may then be written as

$$(b/t)_{cr} = 190/\sqrt{F_y} \qquad (2\text{-}6)$$

For G40.12 steel, with a yield stress of 44ksi. the critical b/t ratio is 29. The most slender flanged "I" or "WF" section available in Canada, a 6WF15.5, has a b/t ratio of 22.3. This implies, therefore, that all available "I" and "WF" sections will not buckle locally in the elastic range.

2.2 POST-ELASTIC PLATE BUCKLING

One of the earliest solutions to the problem of post-elastic plate buckling, by Bleich (4), considers yielding but not strain-hardening. The plate buckling stress is given simply and conservatively

by

$$F_{cr} = k\pi^2 \frac{E\sqrt{\gamma}}{12(1-\mu^2)}\left(\frac{t}{b}\right)^2 \qquad (2\text{-}7)$$

where $\gamma = E_t/E$. The solution to EQUATION (2-7) is normally of the form $F_{cr}/\sqrt{\gamma}$ being equal to a value. From tabulated values it is then possible to obtain F_{cr}. As the ratio $F_{cr}/\sqrt{\gamma}$ increases, F_{cr} becomes asymptotic to the yield stress of the material, F_y.

The material is heterogeneous during the yielding process with yielding taking place in localized slip bands in which the strain jumps from its value at the elastic limit to that at the outset of strain-hardening. The material is again homogeneous when it has all been strained to the strain-hardening range.

On the basis of orthotropic behaviour, Haaijer (5) derived expressions for the buckling strength of steel plates which predict the strain at buckling, for strains exceeding the elastic limit. He considered a rectangular plate subjected to uniform compressive stresses in one direction large enough to produce strain-hardening. Due to strain-hardening changes may occur in the values of the tangent moduli E_x and E_y, Poisson's ratio μ_x and μ_y, and shear modulus G_t.

Based on relations between increments of strain and stress, the bending and twisting moments in terms of the deflection, ω, can be written as

$$M_x = \frac{-E_x I}{1-\mu_x\mu_y}\left(\frac{\partial^2\omega}{\partial x^2} + \mu_y \frac{\partial^2\omega}{\partial y^2}\right)$$

$$M_y = \frac{-E_y I}{1-\mu_x\mu_y}\left(\frac{\partial^2\omega}{\partial y^2} + \mu_x \frac{\partial^2\omega}{\partial x^2}\right)$$

$$M_{xy} = -2G_t I \frac{\partial^2 \omega}{\partial x \partial y}$$

where $I = t^3/12$.

The equilibrium of the bent plate can be expressed by the differential equation

$$D_x \frac{\partial^4 \omega}{\partial x^4} + 2H \frac{\partial^4 \omega}{\partial x^2 \partial y^2} + D_y \frac{\partial^4 \omega}{\partial y^4} = \frac{-t f_x}{I} \frac{\partial^2 \omega}{\partial x^2} \qquad (2\text{-}8)$$

where

$$D_x = \frac{E_x}{1-\mu_x \mu_y} \qquad D_y = \frac{E_y}{1-\mu_x \mu_y}$$

$$D_{xy} = \frac{\mu_y E_x}{1-\mu_x \mu_y} \qquad D_{yx} = \frac{\mu_x E_y}{1-\mu_x \mu_y}$$

$$2H = D_{xy} + D_{yx} + 4G_t$$

This differential equation, (2-8), can be solved if H^2 is assumed equal to $D_x D_y$, an assumption originally made by Bleich.

The value of f_x at which bifurcation of the initially perfectly plane plate occurs can be determined from EQUATION (2-8). This condition can also be expressed in terms of work, with the additional work done by the external forces due to bending of the plate being equal to the change in internal energy in the plate. This results in the integral equation

$$\frac{f_x t}{I} \iint \left(\frac{\partial \omega}{\partial x}\right)^2 dx\, dy = \iint \left[D_x \left(\frac{\partial^2 \omega}{\partial x^2}\right)^2 + \left(D_{xy} + D_{yx}\right) \left(\frac{\partial^2 \omega}{\partial x^2}\right)\left(\frac{\partial^2 \omega}{\partial y^2}\right) + 4G_t \left(\frac{\partial^2 \omega}{\partial x \partial y}\right)^2 \right] dx\, dy \qquad (2\text{-}9)$$

If external restraints exist along the plate edges, additional terms, representing the work done by the restraints, must be introduced in the right-hand side of EQUATION (2-9). Approximate solutions can be

obtained by assuming the shape of the deflected surface.

The deflection surface for a rectangular plate loaded in compression in the x direction and with one unloaded edge free and the other restrained against rotation (conditions similar to those occurring in the flange of an "I" section) may be considered as

$$\omega = \left[A\frac{y}{b} + B\left\{\left(\frac{y}{b}\right)^2 + a_1\left(\frac{y}{b}\right)^3 + a_2\left(\frac{y}{b}\right)^4\right\}\right] \sin\frac{\pi x}{\ell} \qquad (2\text{-}10)$$

The ratio $\beta = B/A$ depends on the degree of restraint.

Substituting (2-10) in (2-9) and integrating gives

$$f_x = \frac{t^2}{12b^2}\left[D_x\left(\frac{\pi b}{\ell}\right)^2 + D_y\left(\frac{\ell}{\pi b}\right)^2\left(\frac{2\beta + \beta^2 c_3}{1/3 + \beta c_1 + \beta^2 c_2}\right)\right.$$

$$- \left(D_{xy} + D_{yx}\right)\left(\frac{\beta c_4 + \beta^2 c_5}{1/3 + \beta c_1 + \beta^2 c_2}\right)$$

$$\left. + 4G_t\left(\frac{1 + \beta c_6 + \beta^2 c_7}{1/3 + \beta c_1 + \beta^2 c_2}\right)\right]$$

F_{cr}, the minimum value of f_x, is obtained for

$$\frac{\ell}{b} = \pi \sqrt[4]{\frac{1/3 + \beta c_1 + \beta^2 c_2}{2\beta + \beta^2 c_3}} \quad \sqrt[4]{\frac{D_x}{D_y}}$$

For the most conservative case, that represented by $\beta = 0$ (one unloaded edge free and the other hinged), the equation for the critical stress becomes

$$F_{cr} = 4\left(\frac{t}{b}\right)^2\left[\frac{\pi D_x}{12}\left(\frac{b}{L}\right)^2 + G_t\right] \qquad (2\text{-}11)$$

Haaijer suggested the following properties based upon theoretical and experimental investigations

$D_x = 3000$ ksi $\qquad\qquad$ $D_y = 32800$ ksi

$$D_{xy} = D_{yx} = 8100 \text{ ksi} \qquad G_t = 2400 \text{ ksi}$$

According to Haaijer, the yield stress of the material has little effect on the above values.

Lay (6) proposed a solution to the problem of local buckling which eliminates some of the empiricism present in Haaijer's solution. It is assumed that the flange is restrained against buckling by a torsion spring (FIGURE 2-2a) representing the effect of the web. For this case the torsional buckling equation is

$$P = \frac{1}{\bar{r}_o^2}\left[G_t K_t + \left(\frac{n\pi}{L}\right)^2 E_{st}\, I_\omega + k_s\left(\frac{L}{n\pi}\right)^2\right] \qquad (2\text{-}12)$$

where n = an integer; L/n = half wavelength of the buckle; I_ω is the warping constant; K_t is the uniform torsion constant; and k_s is the spring constant of the rotational spring. In EQUATION (2-12)

$$I_\omega = \frac{7}{16}\left(\frac{b^3 t^3}{144}\right)$$

$$G_t = \frac{2G_e}{1 + \frac{E/E_{st}}{4(1+\mu)}} \qquad (2\text{-}13)$$

The spring constant, k_s, can be assessed by considering the resistance of the web to a rotation of the compression flange. Assuming a deformed shape as shown FIGURE 2-2b with no rotation of the tension flange and no relative deflection of the two sides of the compression flange, the value of k_s is

$$k_s = \frac{G_t w^3}{3(d-2t)}$$

The value of n which will give the smallest value of P, that

is btF_y, is derived from

$$\frac{L}{n\pi} = \sqrt[4]{\frac{E_{st}I_\omega}{k_s}}$$

This can also be written as

$$\ell_b = \frac{L}{n} = \pi \sqrt[4]{\frac{E_{st}I_\omega}{k_s}}$$

where ℓ_b = half wavelength of local buckle.

Substituting values for E_{st}, $I\omega$ and k_s results in

$$\ell_b = \frac{\pi b}{4}\left[\frac{t}{w}\left(\frac{A_w}{A_f}\right)^{\frac{1}{4}}\right]\left[{}^{7}/_{3}\left(\frac{1+\mu}{h'} + {}^{1}/_{4}\right)\right]^{\frac{1}{4}} \qquad (2\text{-}14)$$

Based on EQUATION (2-14) Lay and Galambos (7) proposed a theory for local buckling of the compression flange of beams under moment gradient. From FIGURE 2-3 the length of the yielded region, $2\tau L$, is given by similar triangles as

$$2\tau L = \frac{2(M_{ult} - M_o)\, L}{M_{ult}}$$

or

$$\tau = 1 - M_o / M_{ult}$$

It is necessary for τL to be of sufficient length, $2\ell_b$ for a local buckling wave to form, where ℓ_b is given by EQUATION (2-14). For a beam under moment gradient, one end of the yielded region is adjacent to the elastic part which is relatively stiff, while the other end is adjacent to a load point or connection as shown in FIGURE 2-4. Thus, relatively stiff end restraints are provided and a full wavelength is required for the local buckle to form. Therefore,

$$\tau L = 2\ell_b = \frac{\pi b}{2}\left[\frac{t}{w}\left(\frac{A_w}{A_f}\right)^{\frac{1}{4}}\right]\left[\frac{7}{3}\left(\frac{1+\mu}{h'}\right)+\frac{1}{4}\right]^{\frac{1}{4}}$$

or

$$1 - \frac{M_o}{M_{ult}} = \frac{\pi b}{2}\left[\frac{t}{w}\left(\frac{A_w}{A_f}\right)^{\frac{1}{4}}\right]\left[\frac{7}{3}\left(\frac{1+\mu}{h'}\right)+\frac{1}{4}\right]^{\frac{1}{4}}$$

from which

$$M_{ult} = \frac{M_o}{1 - \frac{\pi b}{2}\left[\frac{t}{w}\left(\frac{A_w}{A_f}\right)^{\frac{1}{4}}\right]\left[\frac{7}{3}\left(\frac{1+\mu}{h'}\right)+\frac{1}{4}\right]^{\frac{1}{4}}} \qquad (2\text{-}15)$$

Generally, the ultimate moment obtained from EQUATION (2-15) will be conservative.

2.3 COMPACT SECTIONS

The limitation on the proportions of the flange based on local buckling considerations can be derived from EQUATIONS (2-11) and (2-13). For a relatively long plate EQUATION (2-11) may be written as

$$F_{cr} = (t/b)^2 (G_t)$$

or

$$(b/t)_{cr} = \sqrt{G_t/F_{cr}} \qquad (2\text{-}16)$$

Upon substitution of $\mu = 0.3$, $G_e = E/2.6$, $E = 29500$ ksi and $h = 40$ in EQUATION (2-13), $G_t = 2610$ ksi. Equating the critical stress to F_y results in

$$(b/t)_{cr} = 52/\sqrt{F_y} \qquad (2\text{-}17)$$

where b is half the total flange width. EQUATION (2-17) implies that if $b/t \leq 52/\sqrt{F_y}$ local buckling of the flange will not occur until the flange is fully yielded.

On the basis of torsional buckling relationships, Lay (6) proposed that for the flange to be fully yielded before local buckling occurs.

$$b/t \leq \sqrt{\frac{12.64}{\varepsilon_y(1 + \frac{h}{5.2})\ (3 + \frac{F_u}{F_y})}}$$

For average values of material properties, this reduces to

$$\frac{b}{t} \leq 54/\sqrt{F_y} \qquad (2\text{-}18)$$

where F_u is considered to be $1.3F_y$.

CSA Standard S16-1969, Steel Structures for Buildings (8) requires that flanges subject to compression involving plastic hinge rotation under ultimate load have a width-thickness ratio no greater than $54/\sqrt{F_y}$.

2.4 IN-PLANE BEHAVIOUR OF STEEL BEAMS

FIGURES 2-5 and 2-6 illustrate two possible cases of loading, one resulting in a region of uniform maximum moment, the other producing a moment gradient throughout the span. For both types of loading, the moment-curvature relationship is linear up to the moment at first yield of the compression flange (M_o). Above M_o, curvature increases more rapidly with increase in moment as yielding penetrates through the flange into the web with the moment approaching the plastic moment value. At this point the moment-curvature response for the two cases of loading begin to differ. For the beam under uniform moment, the moment becomes asymptotic to the plastic moment value (M_p). The compression flange is now completely yielded over an

appreciable length and it is possible for a local buckle to form.

For the moment gradient case, moment values greater than M_p are attained due to the presence of strain-hardening. As the moment rises above M_p, the yielded zone of the compression flange lengthens until it reaches a length sufficient to cause local buckling.

2.5 STRESS-STRAIN RELATIONSHIPS

In establishing the moment-curvature relationships up to ultimate moment conditions, it is necessary to employ the stress-strain relationships for the material. The basic stress-strain diagram for structural carbon steel is shown in FIGURE 2-7. Three basic regions are shown up to ultimate stress: (1) elastic, (2) plastic and (3) strain-hardening. The strain-hardening modulus, E_{st}, is defined as shown in FIGURE 2-8. As the actual value of E_{st} varies non-linearly with increase in strain (FIGURE 2-7), use of the idealized value will result in calculated values of curvature being less than actual values if the ultimate moment is based on EQUATION (2-15). The effect of residual stresses does not appear in the stress-strain diagram.

A cross-section containing residual stresses, has certain fibers yielding before others when load is applied to the section. Therefore the section is no longer homogeneous. This results in some difficulty in obtaining theoretical moment-curvature relationships.

The effect of residual stress and strain-hardening, in a

flange subjected to moment gradient, may be approximated by employing a modified stress-strain diagram as shown in FIGURE 2-9. The modified relationship attempts to describe the average behaviour of the section. The elastic range is followed by a range in which the material undergoes the effects of yielding and strain-hardening. The modified modulus E'_{st} is less than the strain-hardening modulus E_{st} and its value may be obtained from the moment-curvature relationships established by tests. For a beam under moment gradient (FIGURE 2-6), the slope of the moment-curvature diagram above M_p equals E'_{st}, where I is the moment of inertia of the section.

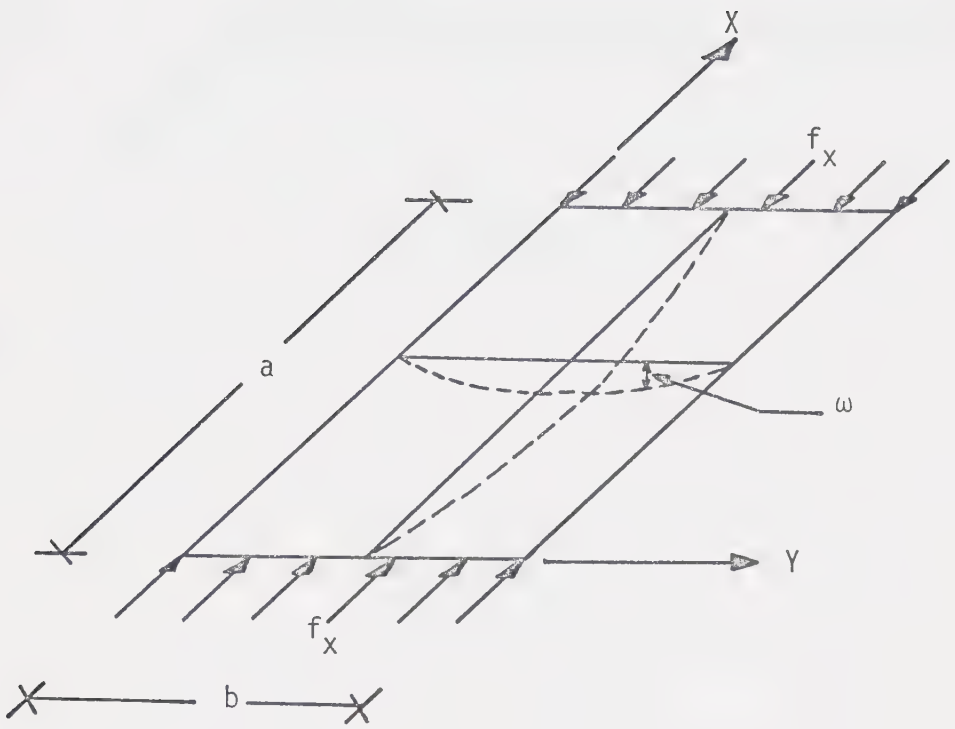

FIGURE 2-1 BUCKLED PLATE

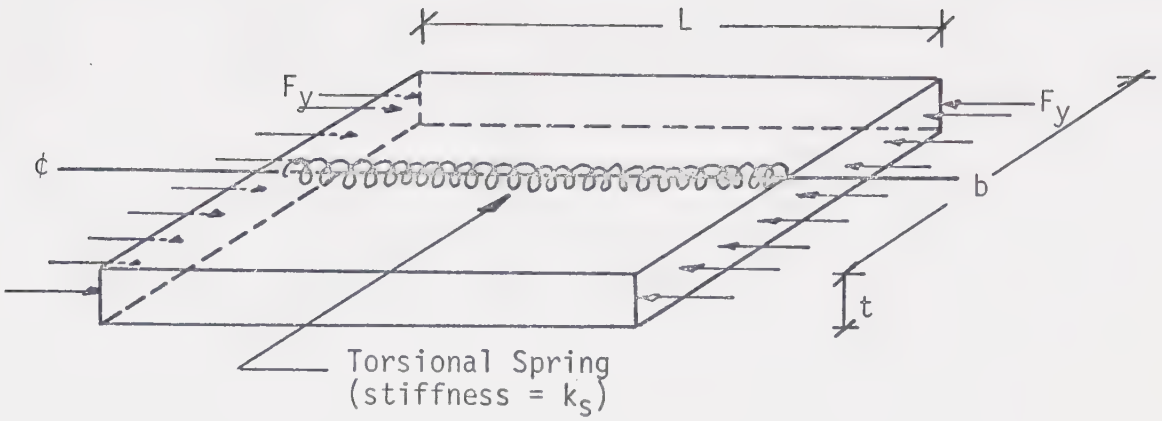

(a) Flange Model

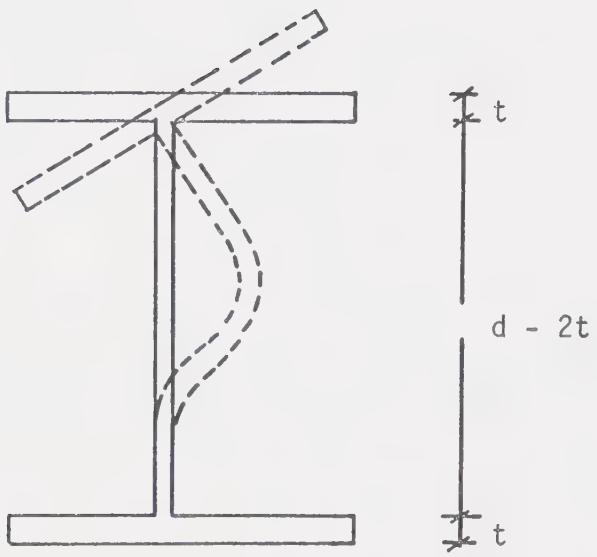

(b) Assumed Deformed Shape

FIGURE 2-2 FLANGE BUCKLING MODEL

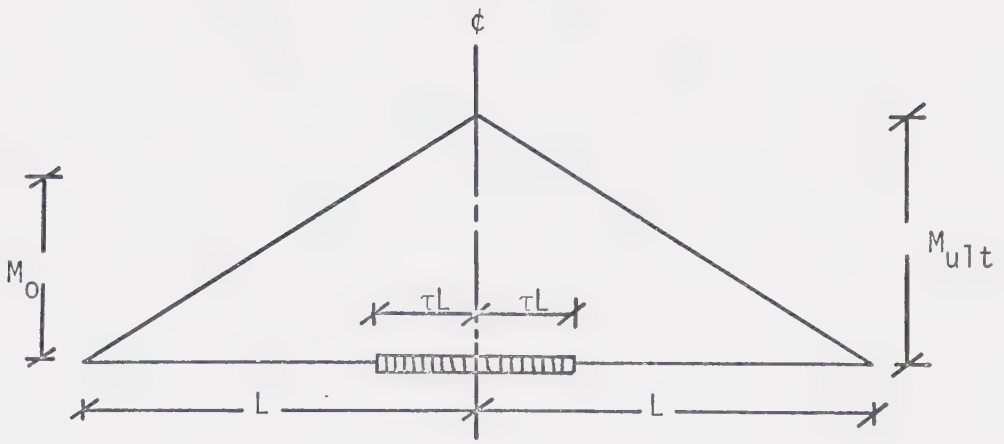

FIGURE 2-3 BENDING MOMENT DIAGRAM

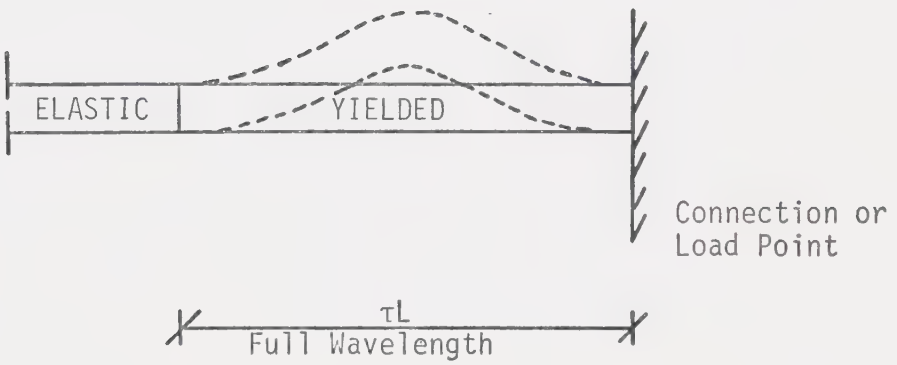

FIGURE 2-4 SHAPE OF LOCAL BUCKLE

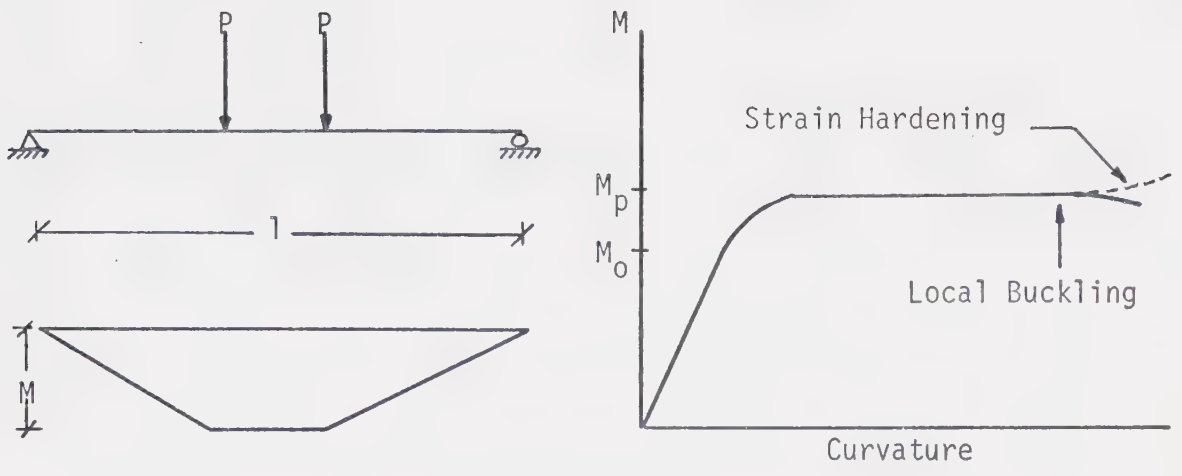

FIGURE 2-5 BEHAVIOUR OF A LATERALLY SUPPORTED BEAM UNDER UNIFORM MOMENT

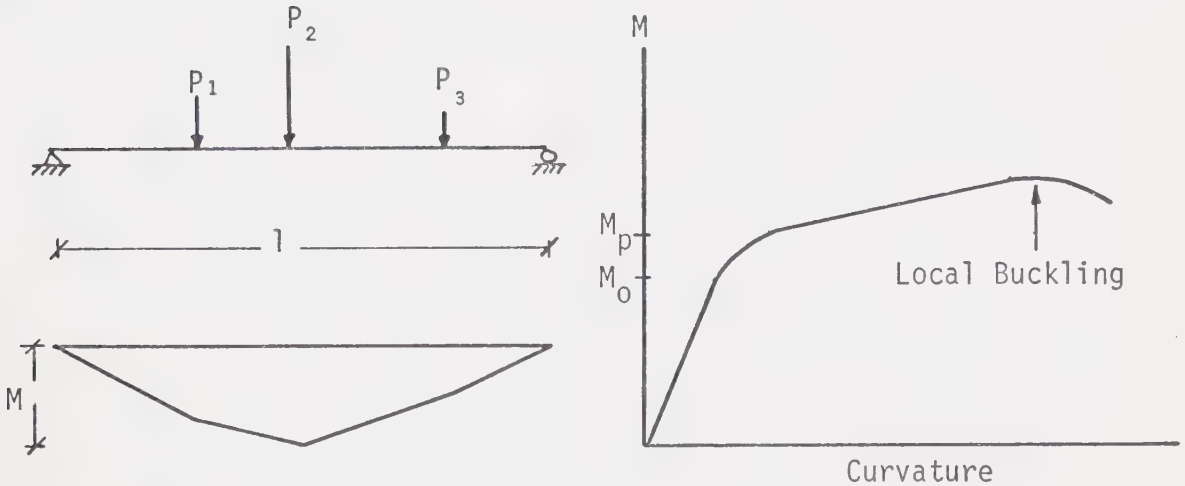

FIGURE 2-6 BEHAVIOUR OF A LATERALLY SUPPORTED BEAM UNDER MOMENT GRADIENT

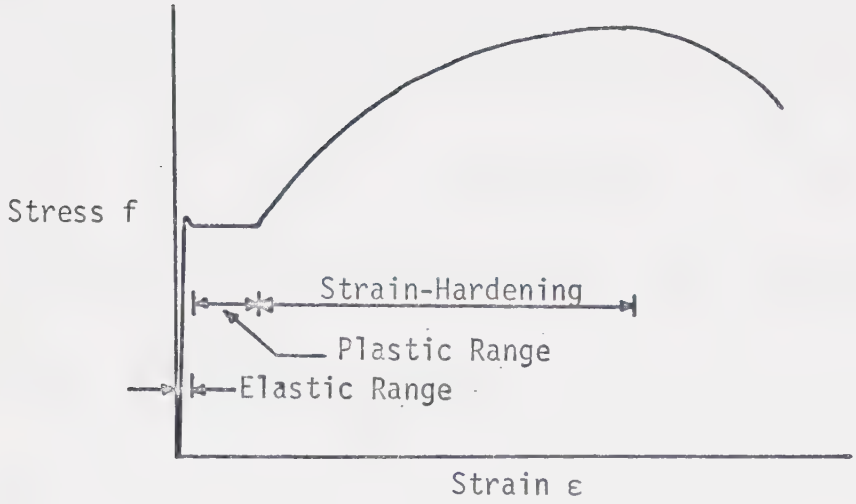

FIGURE 2-7 STRESS-STRAIN DIAGRAM FOR STRUCTURAL CARBON STEEL

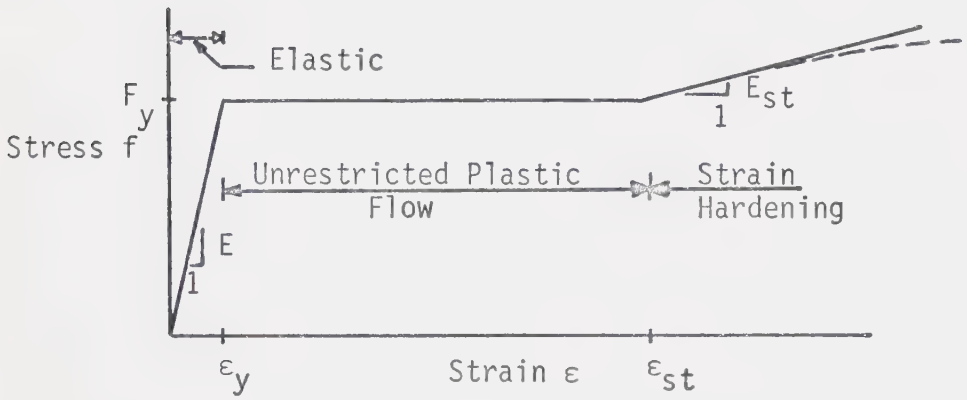

FIGURE 2-8 IDEALIZED STRESS-STRAIN DIAGRAM

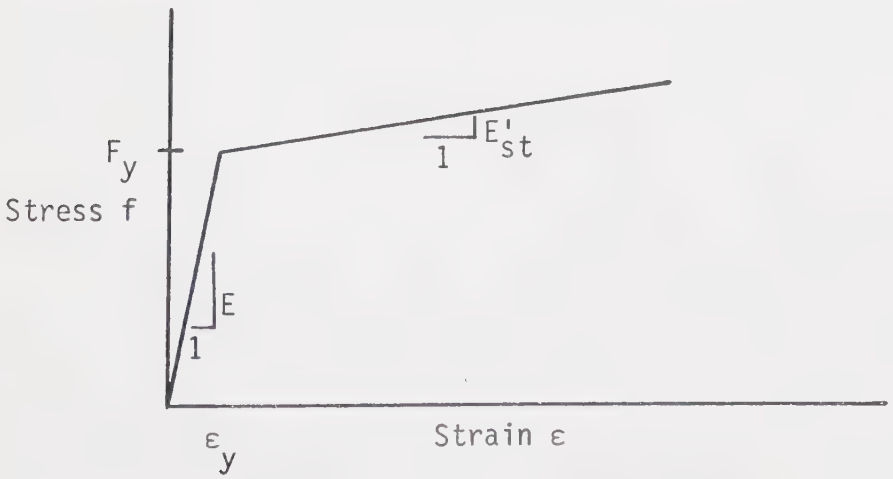

FIGURE 2-9 MODIFIED STRESS-STRAIN DIAGRAM

CHAPTER III

THEORETICAL ANALYSIS OF COMPOSITE BEAMS IN NEGATIVE BENDING

3.1 BEHAVIOUR OF COMPOSITE BEAMS IN NEGATIVE BENDING

FIGURE 3-1 illustrates the general behaviour in terms of the moment-curvature relationship for composite beams tested in negative bending at the University of Alberta. Initially curvature increases in direct proportion to the moment. Beyond a moment value, M_o, curvature increases more rapidly as the midspan moment approaches the plastic moment value, M_p. Further increases in moment is produced by strain-hardening. Local buckling of the web or compression flange at ultimate moment, M_{ult}, results in unloading of the section with further increase in curvature. The moment-curvature relationship for composite beams in negative bending is, therefore, similar to that illustrated previously for plane steel beams under moment gradient.

Since in negative bending, the compression flange is not in contact with the concrete slab, it behaves in a manner similar to the compression flange for a plane "I" or "WF" section. The concrete transfers shear from the shear connectors to the longitudinal slab reinforcement, but does not contribute to the flexural strength of the composite section except for very low loads. The location of the neutral axis depends on the amount of longitudinal slab reinforcement. As loading is increased, inelastic behaviour is initiated in the compression flange and the neutral axis moves from the centroid of

the section towards the tension flange.

3.2 BASIC ASSUMPTIONS FOR THEORETICAL ANALYSIS

It is assumed that a linear strain distribution exists over the entire section as shown in FIGURE 3-2. To account for possible slip between the steel section and the concrete slab, it is assumed that the longitudinal slab reinforcement yields but does not strain sufficiently to strain-harden. From experimental results (2) and (3) it has been established that the longitudinal slab reinforcement yields prior to ultimate conditions if the number of shear connectors is sufficient to develop the ultimate moment.

From experimental results (3) it appears that there is an upper limit to the ultimate moment regardless of the amount of longitudinal slab reinforcement. Additional area of longitudinal reinforcement beyond the area required to place the neutral axis in the tension flange results in no appreciable increase in ultimate moment. While the section is elastic the neutral axis is located at the centroid of the section. The initiation of inelastic action in the compression flange, due to moment values greater than M_o, results in the neutral axis moving towards the tension flange. However, once strain-hardening of the compression flange begins the neutral axis migrates towards the compression flange. Therefore, the neutral axis is located closest to the tension flange for a moment value between M_o and M_p. Assuming that the critical moment value is M_p, the amount of slab reinforcement which effectively contributes to the flexural strength of the composite section is, from FIGURE 3-3

$$A_s \leq \frac{(hw)\ (F_{yw})}{(F_{ys})} \qquad (3\text{-}1)$$

where F_{yw} = yield stress of web, F_{ys} = yield stress of longitudinal slab reinforcement, hw = area of web and A_s = area of longitudinal slab reinforcement. In the theoretical analysis, if the neutral axis at M_p falls in the tension flange, the amount of longitudinal slab reinforcement is reduced to the amount corresponding to a neutral axis location at the inner face of the tension flange.

The expression for the web spring constant, k_s, given by Lay (6) may be modified to account for the strain distribution present in the web. Lay assumed that the web had fully yielded under the longitudinal stresses present. When local buckling of the compression flange occurs, only the compressed part of the web is affected as shown in FIGURE 3-4. As the tension zone of the web is stiff relative to the compression zone of the web, it is reasonable to assume that the compressed portion of the web acts as a propped cantilever as shown in FIGURE 3-4. Assuming the plate to be fixed at the location of the neutral axis, the spring constant expressing the restraint offered by the web is

$$k_s = \frac{G_t w^3}{3z} \qquad (3\text{-}2)$$

where z is the distance to the neutral axis from the compression flange, w is the thickness of the web and G_t is the inelastic shear modulus. Thus, k_s is actually a function of load for composite sections. However, for simplicity, z is assumed to correspond

to the neutral axis location at moment M_o.

3.3 PROCEDURE FOR OBTAINING THEORETICAL MOMENT-CURVATURE RELATIONSHIPS

The moment at first yield of the compression flange, M_o, is required when solving for M_{ult} by using EQUATION (2-15)

$$M_{ult} = \frac{M_o}{1 - \frac{\pi b}{2}\left[\frac{t}{w}\left(\frac{A_w}{A_f}\right)^{\frac{1}{4}}\right]\left[\frac{7}{3}\left(\frac{1+\mu}{h'} + \frac{1}{4}\right)\right]^{\frac{1}{4}}}$$

The value of M_o can be obtained from equilibrium considerations, with the amount of longitudinal slab reinforcement equal to or less than the limiting value given by EQUATION (3-1), and the compression flange in the yielded state. An alternate method for determining M_{ult} involves the calculation of M_o and the length of compression flange involved in the formation of a local buckle. FIGURE 3-5 shows how by similar triangles it is then possible to calculate the ultimate moment.

In order to establish one value for the moment-curvature relationship, values for curvature and neutral axis location are assumed. It is then possible to determine the strain distribution over the cross-section. From the stress-strain relation the stress distribution and the resulting forces acting on the section are determined. Summing the forces will indicate whether or not the section is in equilibrium. If the section is not in equilibrium it is necessary to relocate the neutral axis and recalculate the strain distribution, related stresses and forces until equilibrium of the

section is obtained. Once the section is in equilibrium it is a simple matter to obtain the resisting moment corresponding to the assumed curvature. The complete moment-curvature relationship is obtained by repeating the above procedure until the calculated moment equals the moment at which local buckling of the compression flange occurs.

3.4 TOTAL ROTATION AND CENTRELINE DEFLECTION

Once the moment-curvature relationship is established, the total rotation and centreline deflection of the beam may be obtained by the moment-area method. Two ranges must be considered: (1) the entire beam in the elastic range, (2) a portion of the beam in the post-elastic range. FIGURE 3-6 shows the bending moment and curvature diagrams for the two conditions for the type of loading used in the University of Alberta tests.

A) Entire span in elastic range ($\phi \leq \phi_o$)

1) Total rotation:

$$\theta_{total} = \phi(L - \ell)$$

2) Centreline deflection:

$$\delta_{\text{¢}} = \phi/24\ (3L^2 - 4\ell^2)$$

B) Post-elastic case, idealized stress-strain diagram ($\phi > \phi_o$)

1) Total rotation

$$\theta_{total} = \theta\ (\ell + \ell' - x) + \phi(L - 2\ell + x) + \theta\ (x) + 2 \int_{\phi = \phi_o}^{\phi = \phi'} \phi d\ell'$$

2) Centreline deflection:

$$\delta_{\text{¢}} = \frac{\phi_o}{6}(2\ell^2 - \ell'^2 + 2x^2 + 2\ell\ell' - 4\ell x - 2\ell' x)$$

$$+ \frac{\phi}{8}p(4\ell x - 2x^2) + \frac{\phi}{8}(L^2 - 4\ell^2 + 2x^2 + 4\ell x - 4x^2)$$

$$+ \int_{\phi = \phi_o}^{\phi = \phi'} \phi \bar{x} d\ell'$$

C) Post-elastic case, modified stress-strain diagram ($\phi > \phi_o$)

1) Total Rotation:

$$\theta_{total} = \phi_o\ (\ell) + \phi(L - 2\ell + \ell' + x)$$

2) Centreline deflection:

$$\delta = \phi_o/6(2\ell^2 - \ell\ell' - \ell x)$$

$$+ \phi/24(3L^2 - 12\ell^2 + 12\ell' + 8x^2 - 8\ell' x - 4\ell'^2)$$

3.5 COMPUTER PROGRAM

A computer program was developed for the calculation of the ultimate moment based on local buckling and values for moment-curvature, moment-rotation and load-deflection relationships. The program, which is described in Appendix A, also computes the simple plastic moment and the limiting area of longitudinal slab reinforcement.

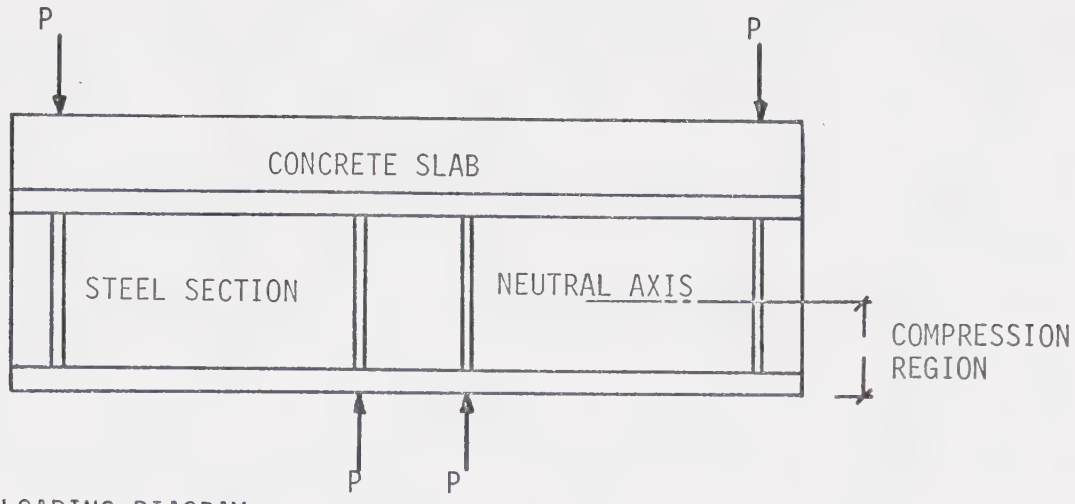

(a) LOADING DIAGRAM

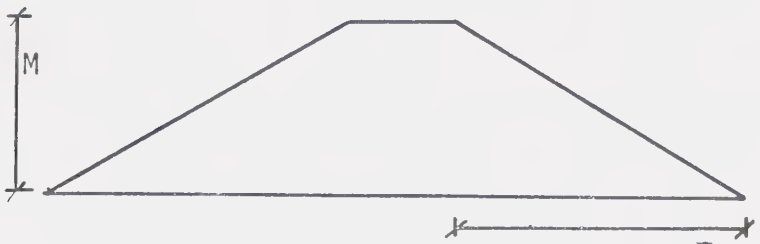

(b) BENDING MOMENT DIAGRAM

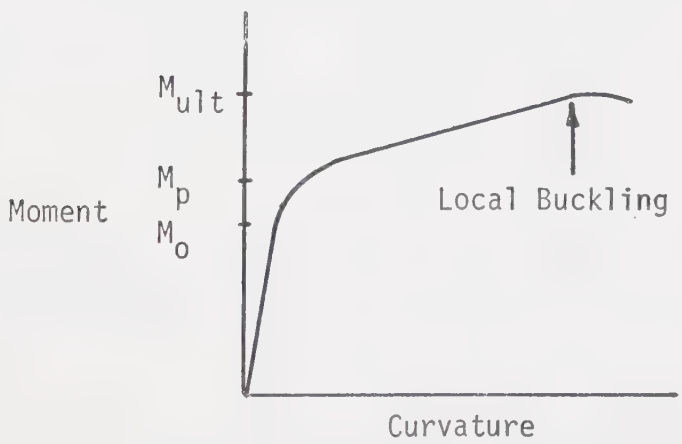

(c) TYPICAL MOMENT CURVATURE DIAGRAM

FIGURE 3-1 UNIVERSITY OF ALBERTA TESTS OF COMPOSITE BEAMS IN NEGATIVE BENDING

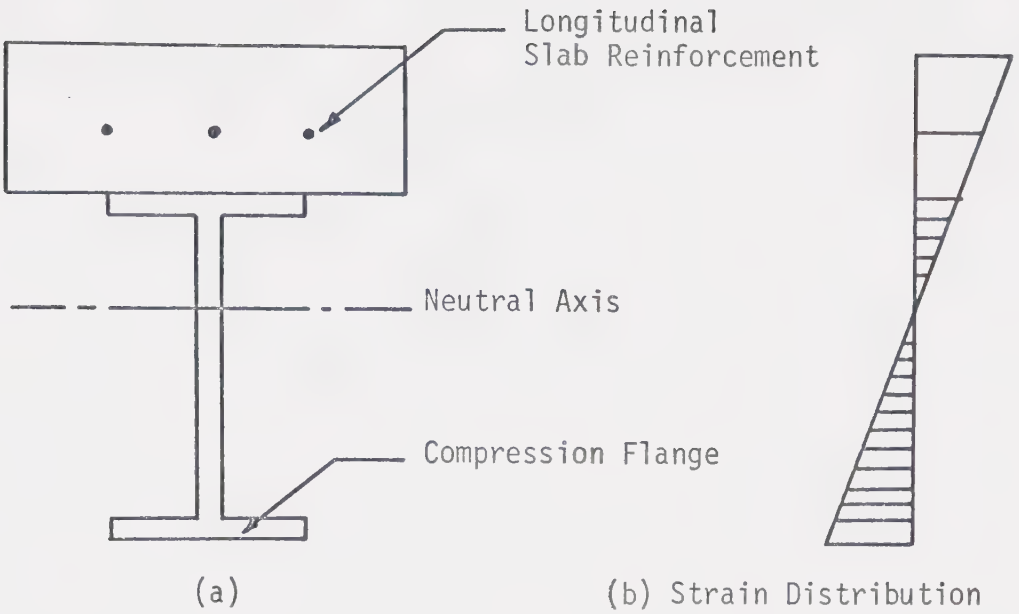

FIGURE 3-2 CROSS-SECTION OF COMPOSITE BEAM IN NEGATIVE BENDING

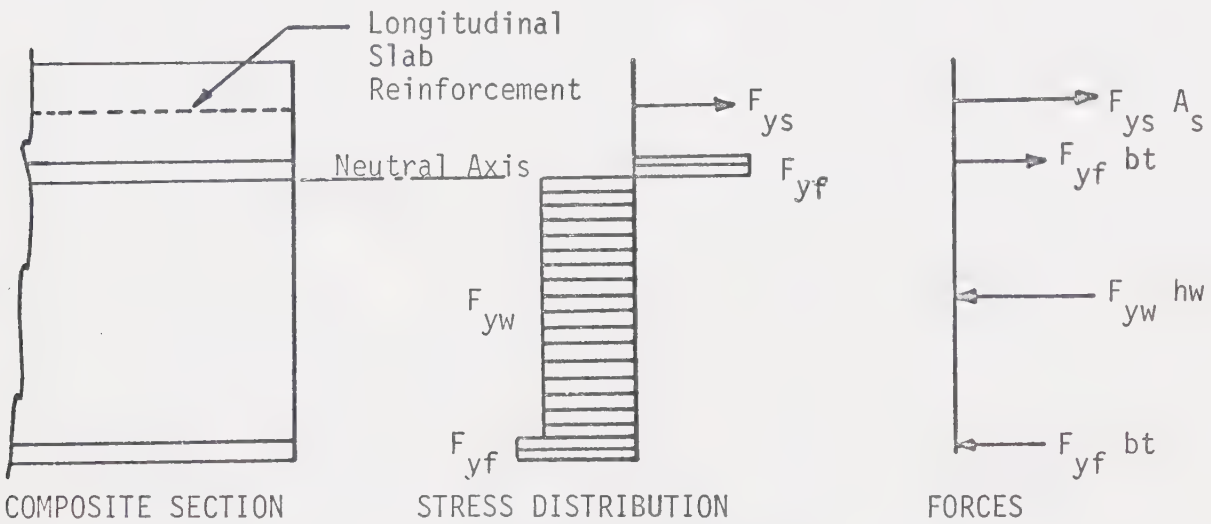

FIGURE 3-3 STRESS DISTRIBUTION CORRESPONDING TO PLASTIC MOMENT WHEN NEUTRAL AXIS IS AT WEB-FLANGE JUNCTION

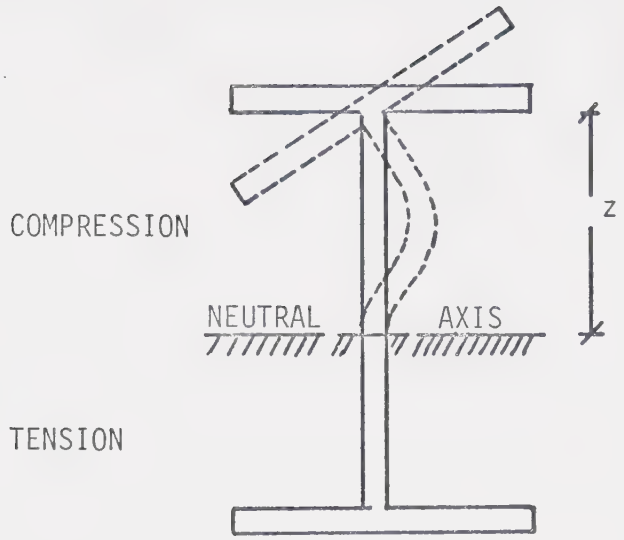

FIGURE 3-4 ASSUMED DEFORMED SHAPE OF CROSS-SECTION FOR DETERMINING SPRING CONSTANT, k_s

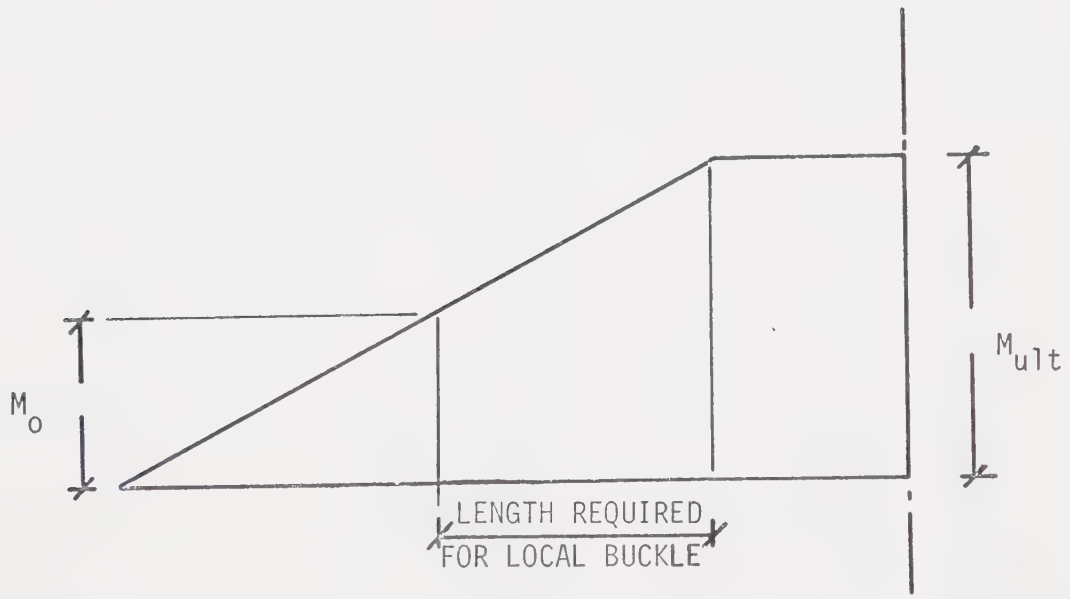

FIGURE 3-5 RELATIONSHIP BETWEEN M_o AND M_{ult}

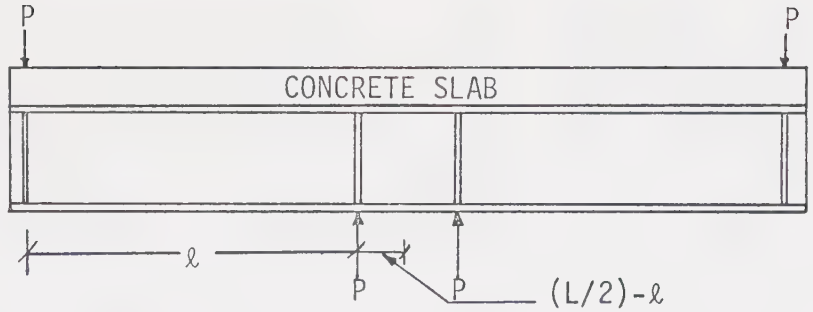

(a) UNIVERSITY OF ALBERTA LOADING

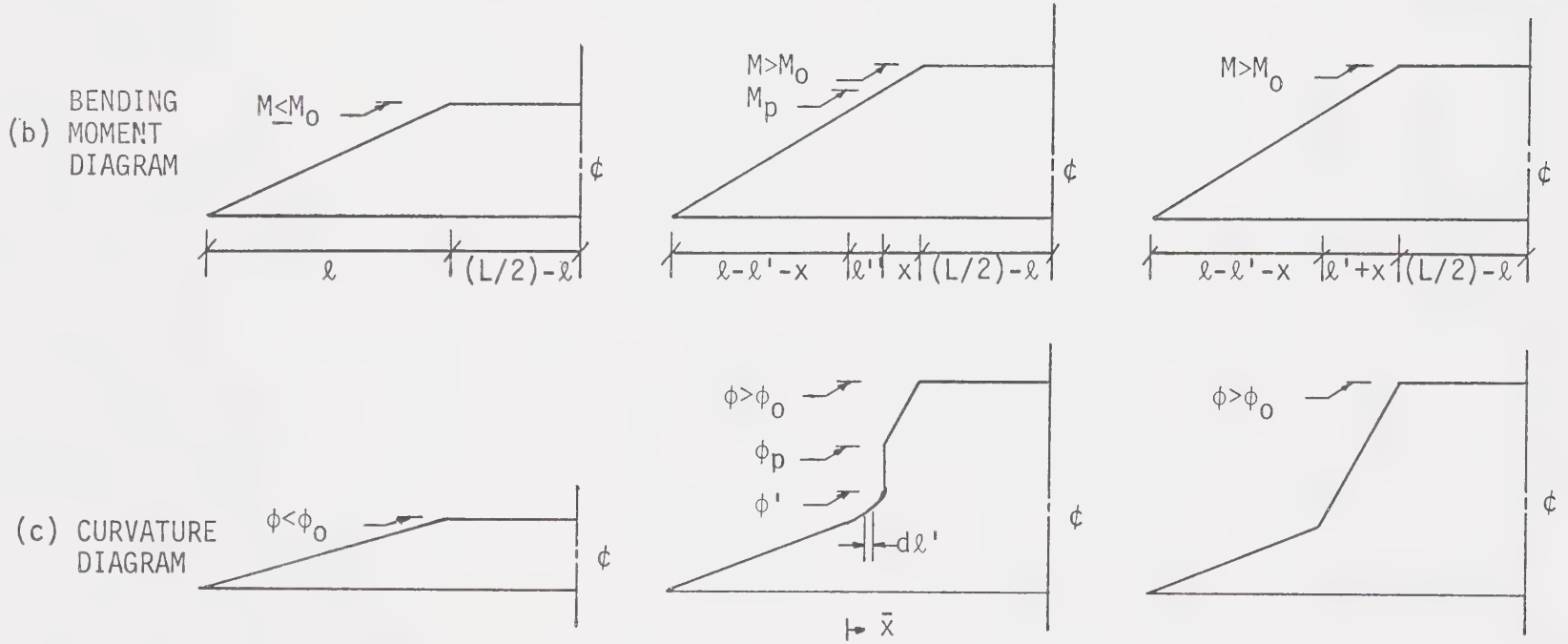

CASE A ENTIRE BEAM ELASTIC

CASE B PORTION OF BEAM INELASTIC (IDEALIZED STRESS-STRAIN DIAGRAM)

CASE C PORTION OF BEAM INELASTIC (MODIFIED STRESS-STRAIN DIAGRAM)

FIGURE 3-6 BENDING MOMENT AND CURVATURE DIAGRAMS

CHAPTER IV

RESULTS

4.1 INTRODUCTION

Experimental results of tests conducted on composite beams in negative bending at the University of Alberta have been presented by previous investigators (2), (3). For comparison purposes, experimental moment-curvature relationships are presented. Theoretical results are presented in graphical and tabular form.

4.2 MATERIAL PROPERTIES

TABLE 4.6 represents results of tensile tests performed on web and flange coupons by previous investigators (2), (3). The yield stress and ultimate stress for the reinforcing bars used in the test beams is also shown.

4.3 GENERAL BEHAVIOUR

The experimental moment-curvature relationships are shown in FIGURES 4-1 and 4-2, while the theoretical relationships, as plotted on the Calcomp plotter, appear in FIGURES 4-3 to 4-6. The theoretical relationship between midspan bending moment and the total rotation of the beam is shown in FIGURES 4-7 and 4-8. Load-deflection relationships are shown in FIGURES 4-9 and 4-10. The location of the neutral axis, with respect to the centroid of the steel section, is plotted against midspan bending moment in FIGURES 4-11 and 4-12.

4.4 ULTIMATE LOAD CONDITIONS

TABLE 4.1 is a summary of experimental results for tests conducted at the University of Alberta by Davison (2) and Lever (1). TABLES 4.2, 4.3, 4.4 and 4.5 summarize the theoretical study. FIGURE 4-13, derived from test data, is a plot of the ratio of ultimate moment of the composite section to ultimate moment of the steel section alone (M_{ult}/M^{o}_{ult}) versus the total tensile force in the longitudinal slab reinforcement at yield ($A_S F_{ys}$). Corresponding values derived from the theoretical study are shown in FIGURE 4-14. FIGURE 4-15 indicates the variation in the ratio of the simple plastic moment for the composite section to the simple plastic moment for the corresponding plain steel section (M_p/M^{o}_p) with total tensile force in the longitudinal slab reinforcement ($A_S F_{ys}$). The effect of varying the b/t ratio on the ultimate capacity of composite beams with constant A_S/A_{WF} ratios is shown in FIGURE 4-16.

SECTION	A_s (in^2)	P_{ult} (Kips)	M_{ult} (Ft. Kips)	ϕ_{ult} ($\frac{Rad}{in.} \times 10^{6}$)	θ_{ult} (Rad$\times 10^{3}$)	δ_{ult} (inches)	M_p (Ft. Kips)
12WF36	--						
(18)	0.00	135	241.9	8325	--	3.48	173.1
(11)	1.18	156	279.6	7900	--	3.12	207.7
(12)	1.96	160	286.7	6500	--	3.20	224.8
(13,16,17)	2.45	162	290.3	4950	--	2.59	233.2
(14,15)	3.68	166	297.5	2500	--	1.84	247.6
12WF31	--						
(21)	0.00	120	215	--	--	2.95	152.8
(22)	0.80	133	238	--	117	2.60	176.9
(23)	1.86	139	249	2550	69	1.43	200.6
(24)	2.48	140	251	--	69	1.15	210.1
(25)	3.72	135	242	800	54	1.12	223.0
12WF27	--						
(31)	0.00	106	189	13800	130	2.3	154.1
(32)	0.80	112	200	3000	66	1.5	177.6
(33)	1.60	120	215	--	40	1.1	196.5
(34)	3.10	126	225.5	1050	30	0.9	218.6
12B16.5	--						
(41)	0.00	46	82.3	1500	57	1.07	77.4
(42)	1.02	62	111.0	1460	32	0.55	106.5
(43)	1.86	67	120.0	1460	29	0.55	122.9

TABLE 4.1 EXPERIMENTAL RESULTS

SECTION	A_s (in^2)	A'_s (in^2)	P_{ult} (Kips)	M_{ult} (Ft. Kips)	ϕ_{ult} ($\frac{Rad}{in.} \times 10^{6}$)	θ_{ult} ($Rad \times 10^{3}$)	δ_{ult} (inches)	M_p (Ft. Kips)
12WF36	--							
	0.00		128.7	230.5	4971	117	3.77	173.1
	1.18		143.7	257.5	4260	89	2.92	207.7
	1.96		150.8	270.2	3596	72	2.39	224.8
	2.45		154.6	277.0	3193	64	2.10	233.2
	3.68	3.06	158.6	284.2	2650	54	1.76	247.6
12WF31	--							
	0.00		114.8	205.8	5528	134	4.25	152.8
	0.80		125.7	224.7	5032	110	3.58	176.9
	1.86		136.0	242.7	4027	81	2.69	200.6
	2.48		140.0	250.8	3389	67	2.24	210.7
	3.72	2.76	141.8	254.1	3019	62	2.02	223.0
12WF27 *	--							
	0.00		104.7	187.6	6739	166	5.20	140.6
	0.80		115.4	206.9	6157	135	4.39	164.1
	1.60		123.1	220.6	5208	105	3.49	181.4
	3.10	2.41	129.4	231.0	3885	79	2.60	199.5
12B16.5	--							
	0.00		44.2	79.1	2937	46	1.57	77.4
	1.02		59.4	98.7	375	16	0.36	106.5
	1.86		68.6	107.6	305	14	0.31	122.9

* Experimental material properties appear in error, values falling between those for 12B16.5 and 12WF31 were therefore used for theoretical results.

TABLE 4.2 THEORETICAL RESULTS
BASED ON IDEALIZED STRESS-STRAIN DIAGRAM AND ACTUAL MATERIAL PROPERTIES

SECTION	A_s (in^2)	A'_s (in^2)	P_{ult} (Kips)	M_{ult} (Ft. Kips)	ϕ_{ult} ($\frac{Rad}{in.} \times 10^{6}$)	θ_{ult} (Rad$\times 10^{3}$)	δ_{ult} (inches)	M_p (Ft. Kips)
12WF36	--							
	0.00		128.7	230.5	3629	80	2.56	173.1
	1.18		143.7	257.5	2970	61	1.97	207.7
	1.96		150.8	270.2	2398	49	1.58	224.8
	2.45		154.6	277.0	2069	43	1.36	233.2
	3.68	3.06	158.6	284.2	1720	37	1.16	247.6
12WF31	--							
	0.00		114.8	205.8	3728	83	2.64	152.8
	0.80		125.7	224.7	3262	68	2.19	176.9
	1.86		136.0	242.7	2411	49	1.58	200.6
	2.48		140.0	250.8	1959	41	1.31	210.7
	3.72	2.76	141.8	254.1	1789	38	1.21	223.0
12WF27 *	--							
	0.00		104.7	187.6	4240	93	2.97	140.6
	0.80		115.4	206.9	3697	76	2.47	164.1
	1.60		123.1	220.6	2900	58	1.89	181.4
	3.10	2.41	129.4	231.0	2163	45	1.44	199.5
12B16.5	--							
	0.00		44.2	79.1	605	21	0.50	77.4
	1.02		59.4	98.7	361	16	0.35	106.5
	1.86		68.6	107.6	299	14	0.31	122.9

* See note TABLE 4.2

TABLE 4.3 THEORETICAL RESULTS
BASED ON MODIFIED STRESS-STRAIN DIAGRAM AND ACTUAL MATERIAL PROPERTIES

SECTION	A_s (in^2)	A'_s (in^2)	P_{ult} (Kips)	M_{ult} (Ft. Kips)	ϕ_{ult} ($\frac{Rad}{in.} \times 10^{6}$)	θ_{ult} ($Rad \times 10^{6}$)	δ_{ult} (inches)	M_p (Ft. Kips)
12WF36	--							
	0.00		142.1	254.7	7587	188	5.92	186.8
	1.18		158.6	284.2	6895	151	4.94	221.3
	1.96		166.4	298.2	6122	126	4.19	238.2
	2.45		170.6	305.7	5595	113	3.76	246.4
	3.68	3.00	174.6	312.8	4990	99	3.32	260.5
12WF31	--							
	0.00		120.7	216.2	7535	186	5.85	159.5
	0.80		132.0	236.5	7014	156	5.07	183.4
	1.86		142.6	255.6	5813	118	3.93	206.4
	2.48		147.3	263.9	5009	99	3.32	215.1
	3.72	2.60	148.1	265.5	4779	95	3.17	227.7
12WF27	--							
	0.00		101.8	182.5	7212	174	5.49	137.5
	0.80		112.6	201.8	6537	140	4.59	160.9
	1.60		120.2	215.3	5441	107	3.60	178.0
	3.10	2.36	125.6	225.0	4099	82	2.71	195.7
12B16.5	--							
	0.00		42.8	76.7	3059	49	1.67	74.0
	1.02		53.1	95.2	345	15	0.33	102.6
	1.86		57.7	103.4	295	14	0.30	118.2

TABLE 4.4 THEORETICAL RESULTS
BASED ON IDEALIZED STRESS-STRAIN DIAGRAM AND SPECIFIED MATERIAL PROPERTIES

SECTION	A_s (in^2)	A'_s (in^2)	P_{ult} (Kips)	M_{ult} (Ft. Kips)	ϕ_{ult} ($\frac{Rad}{in.} \times 10^{-6}$)	θ_{ult} ($Rad \times 10^{-3}$)	δ_{ult} (inches)	M_p (Ft. Kips)
12WF36	--							
	0.00		142.1	254.7	5123	113	3.63	186.8
	1.18		158.6	284.2	4479	90	2.99	221.3
	1.96		166.4	298.2	3805	75	2.48	238.2
	2.45		170.6	305.7	3379	67	2.20	246.4
	3.62	3.00	174.6	312.8	2932	59	1.92	260.5
12WF31	--							
	0.00		120.7	216.2	5055	111	3.56	159.5
	0.80		132.0	236.5	4565	93	3.06	183.4
	1.86		142.6	255.6	3523	69	2.29	206.4
	2.48		147.3	263.9	2917	58	1.91	215.1
	3.72	2.60	148.1	265.5	2811	56	1.84	227.7
12WF27	--							
	0.00		101.8	182.5	4711	102	3.27	137.5
	0.80		112.6	201.8	4081	82	2.68	160.9
	1.60		120.2	215.3	3153	62	3.02	178.0
	3.10	2.36	125.6	225.0	2373	48	1.56	195.7
12B16.5	--							
	0.00		42.8	76.7	663	21	0.52	74.0
	1.02		53.1	95.2	332	15	0.32	102.6
	1.86		57.7	103.4	288	13	0.29	118.2

TABLE 4.5 THEORETICAL RESULTS
BASED ON MODIFIED STRESS-STRAIN DIAGRAM AND SPECIFIED MATERIAL PROPERTIES

SECTION	TYPE	F_y(ksi)	F_u(Ksi)	E(ksi)	ε_{st}(in/in)	E_{st}(ksi)
12WF36	FLANGE	40.4	67.7	29700	0.0057	857
		39.8	67.7	-	0.0081	658
		39.2	67.9	28800	0.0066	725
		39.7	67.8	27600	0.0106	738
	Ave.	39.8	67.8	28700	0.0078	745
	WEB	46.4	69.2	27600	0.0144	-
		43.5	69.2	29400	0.0170	593
	Ave.	45.0	69.2	28500	0.0157	593
12WF31	FLANGE	40.7	69.4	33600	0.0111	722
		41.7	69.6	27800	0.0086	827
		41.0	70.0	29300	0.0115	744
	Ave.	41.1	69.7	30200	0.0104	764
	WEB	47.0	72.5	33600	0.0140	783
		46.4	70.2	32200	0.0156	788
	Ave.	46.7	71.3	32900	0.0148	785
12WF27	FLANGE	48.7	77.2	34700	0.0086	790
		47.8	77.9	29900	0.0060	553
		47.7	79.8	39800	0.0079	805
		49.4	77.0	30800	0.0080	725
	Ave.	48.4	78.0	33800	0.0076	718
	WEB	53.8	79.3	38500	0.0158	725
		52.7	78.0	42000	-	712
	Ave.	53.3	78.6	40250	0.0158	718
12B16.5	FLANGE	43.8	68.0	29200	0.0154	734
		44.9	68.6	28100	0.0160	580
		46.2	68.1	28900	0.0162	553
		45.4	68.1	25200	0.0150	507
	Ave.	45.1	68.2	27800	0.0157	593
	WEB	46.4	69.1	-	0.0186	652
		48.8	69.8	28700	0.0226	580
	Ave.	47.6	69.5	28700	0.0206	616

Average Slab Reinforcement Data

Size	Yield Stress (ksi)	Ultimate Stress (ksi)
#3	52.4	76.2
#4	51.9	78.6
#5	51.7	79.4

TABLE 4.6 ACTUAL MATERIAL PROPERTIES

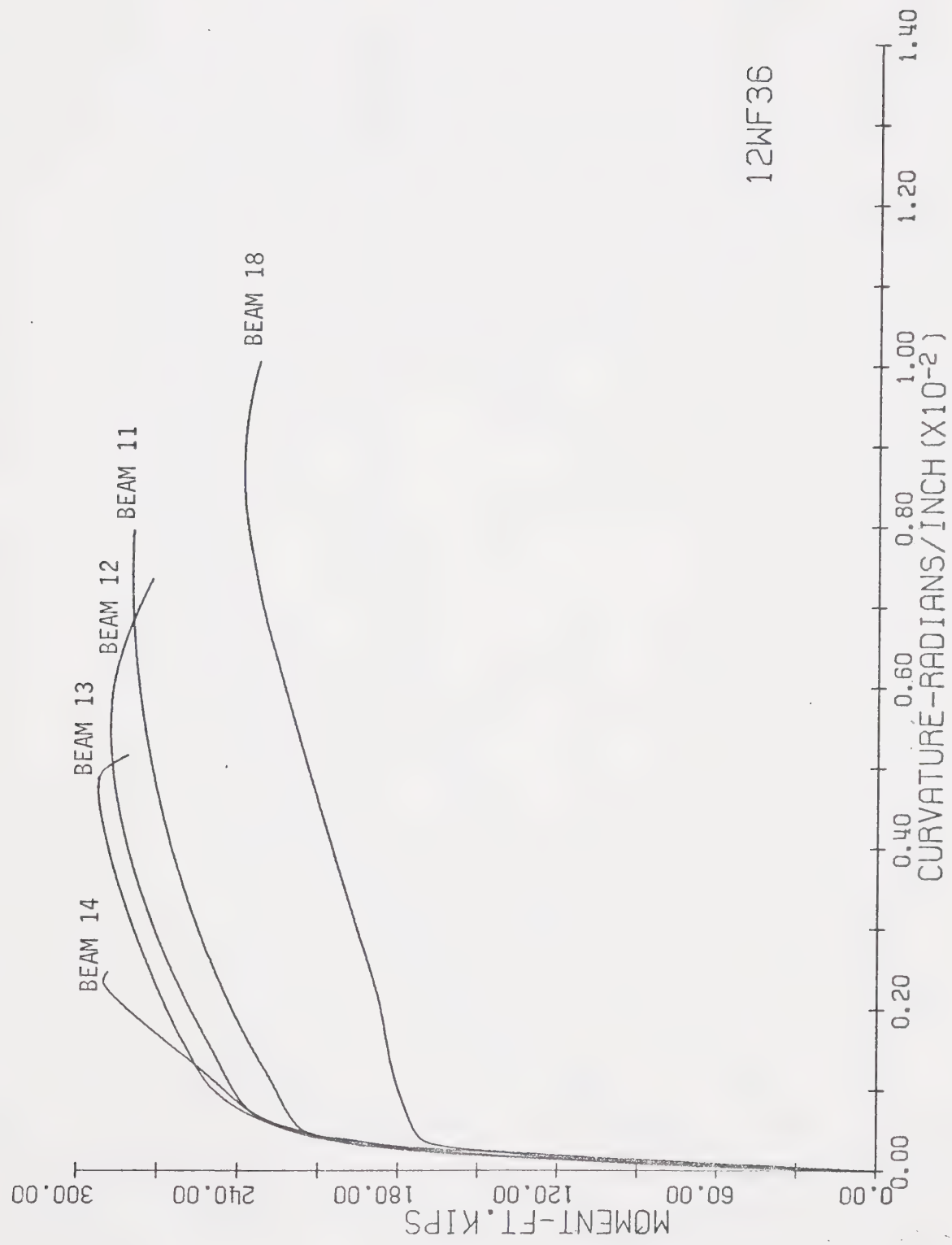

FIGURE 4-1 EXPERIMENTAL MOMENT-CURVATURE DIAGRAM

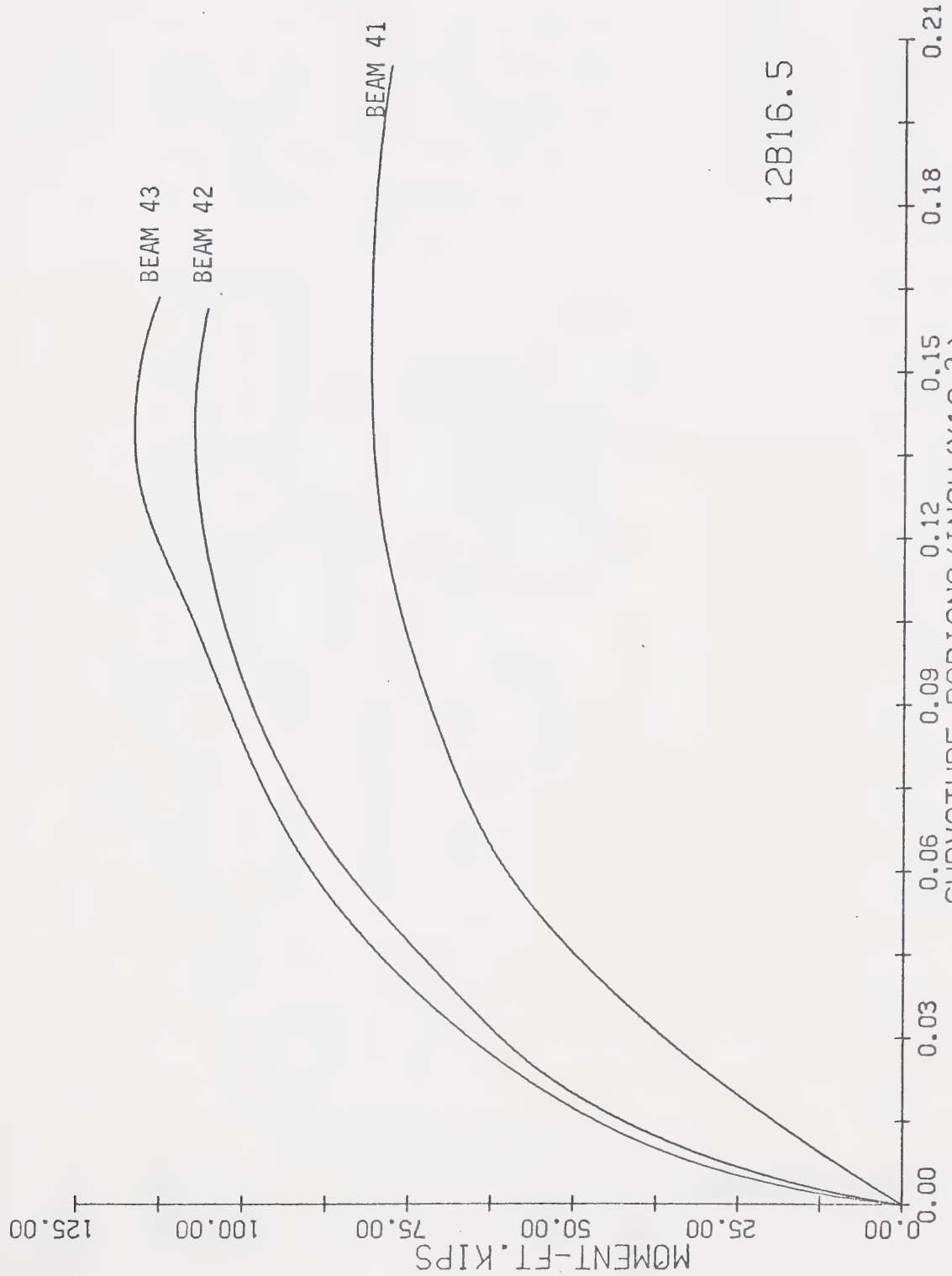

FIGURE 4-2 EXPERIMENTAL MOMENT-CURVATURE DIAGRAM

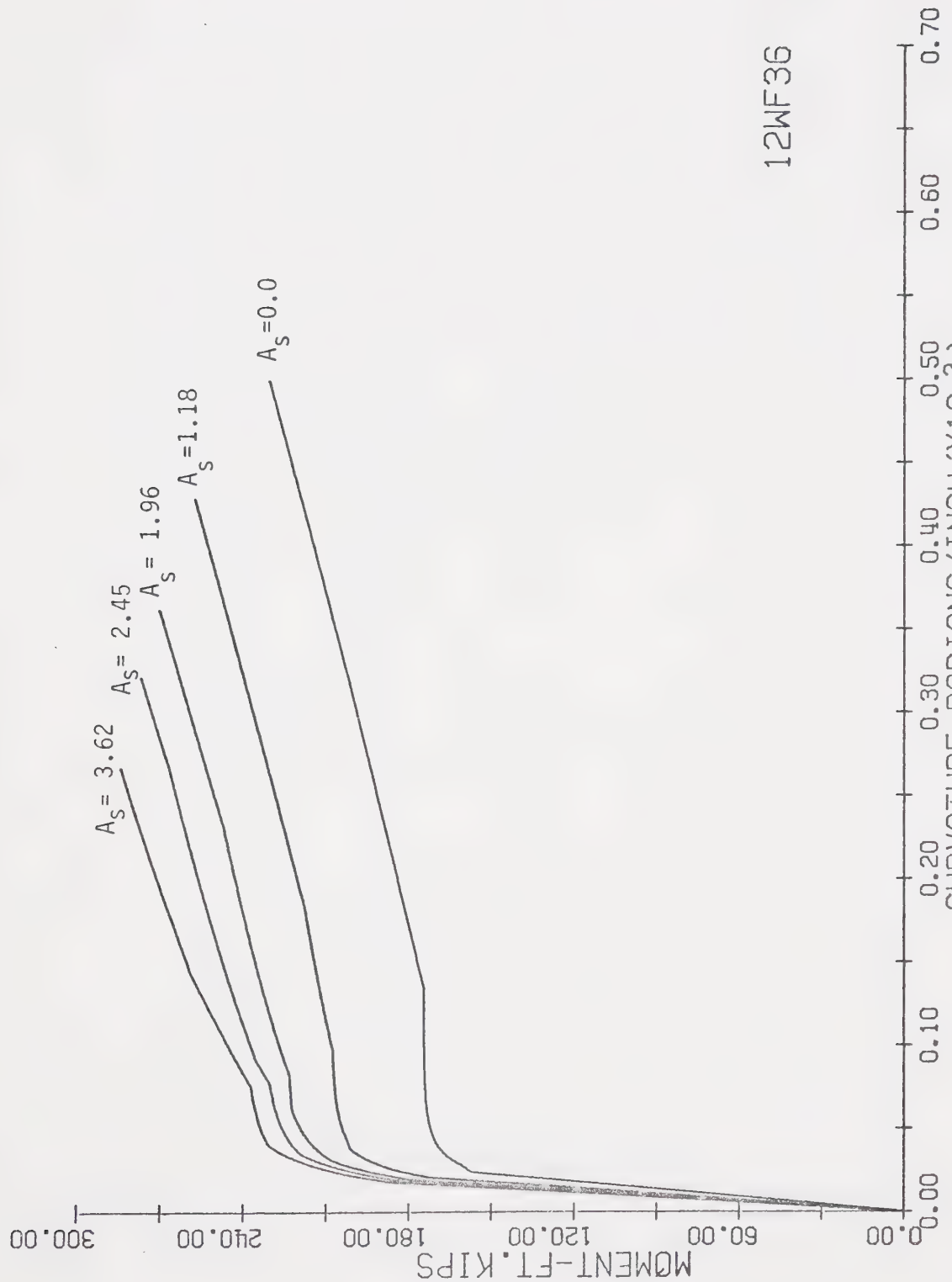

FIGURE 4-3 THEORETICAL MOMENT-CURVATURE DIAGRAM FOR 12WF36 SERIES
(IDEALIZED STRESS-STRAIN DIAGRAM)

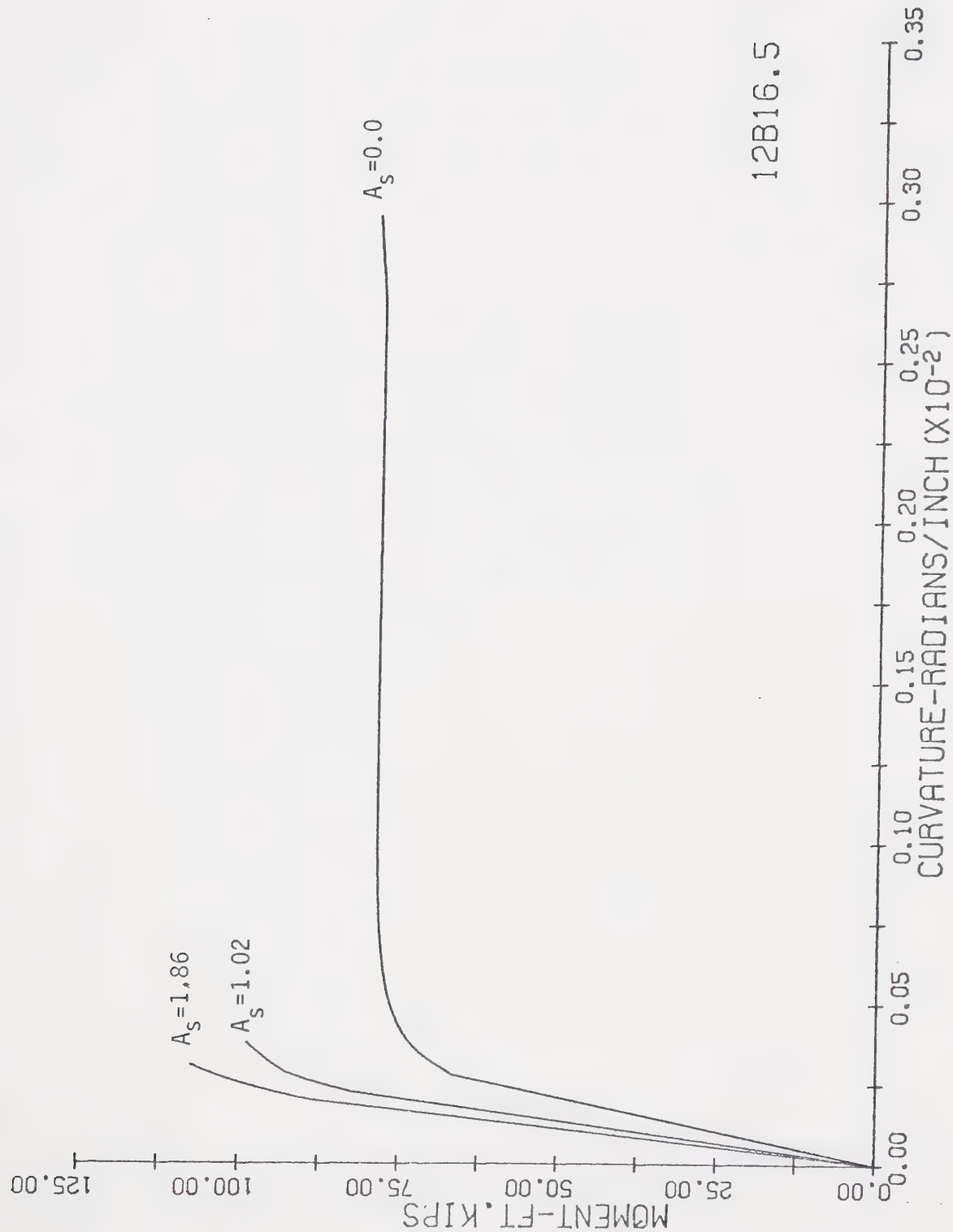

FIGURE 4-4 THEORETICAL MOMENT-CURVATURE DIAGRAM FOR 12B16.5 SERIES
(IDEALIZED STRESS-STRAIN DIAGRAM)

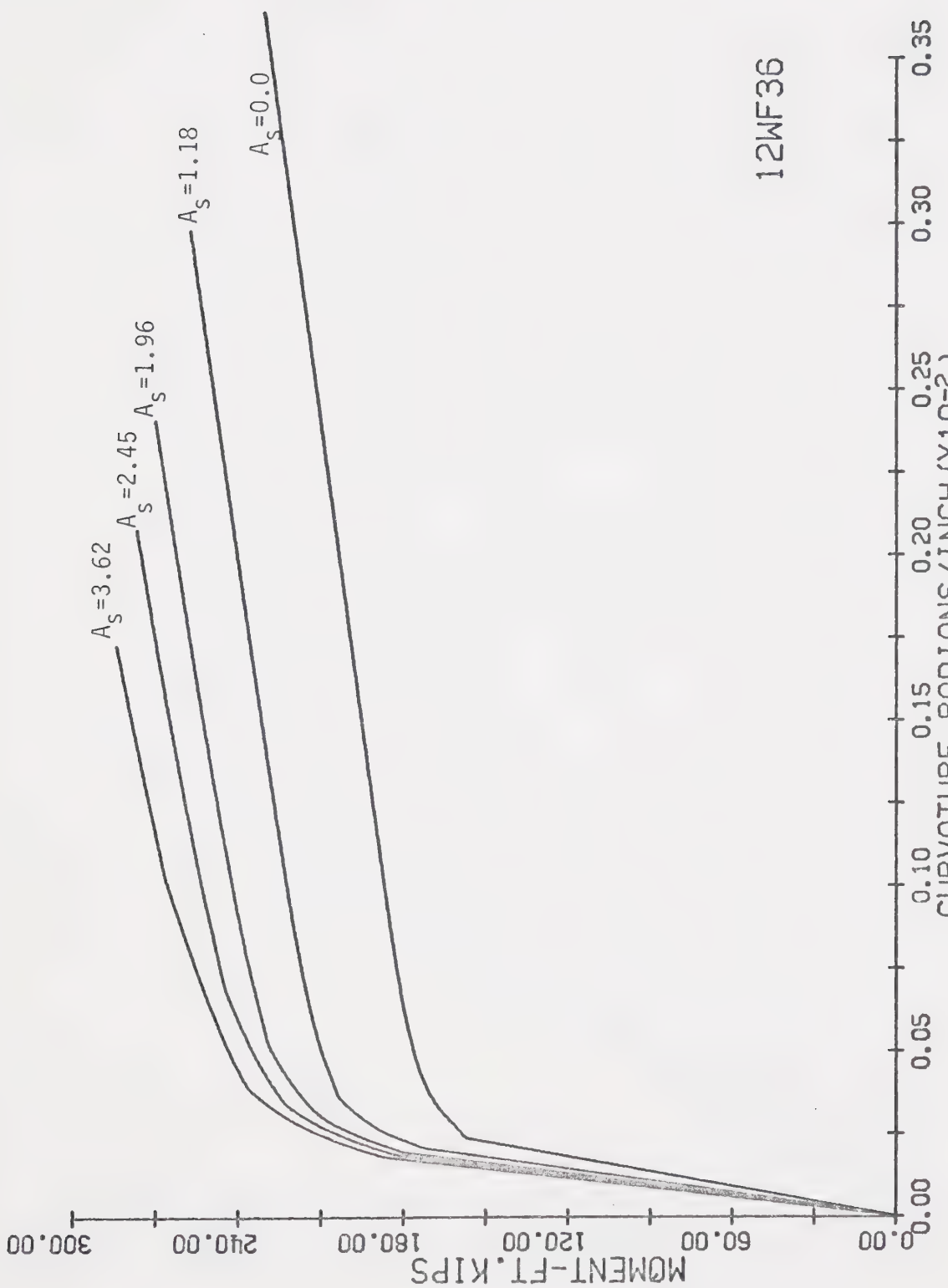

FIGURE 4-5 THEORETICAL MOMENT-CURVATURE DIAGRAM FOR 12WF36 SERIES
(MODIFIED STRESS-STRAIN DIAGRAM)

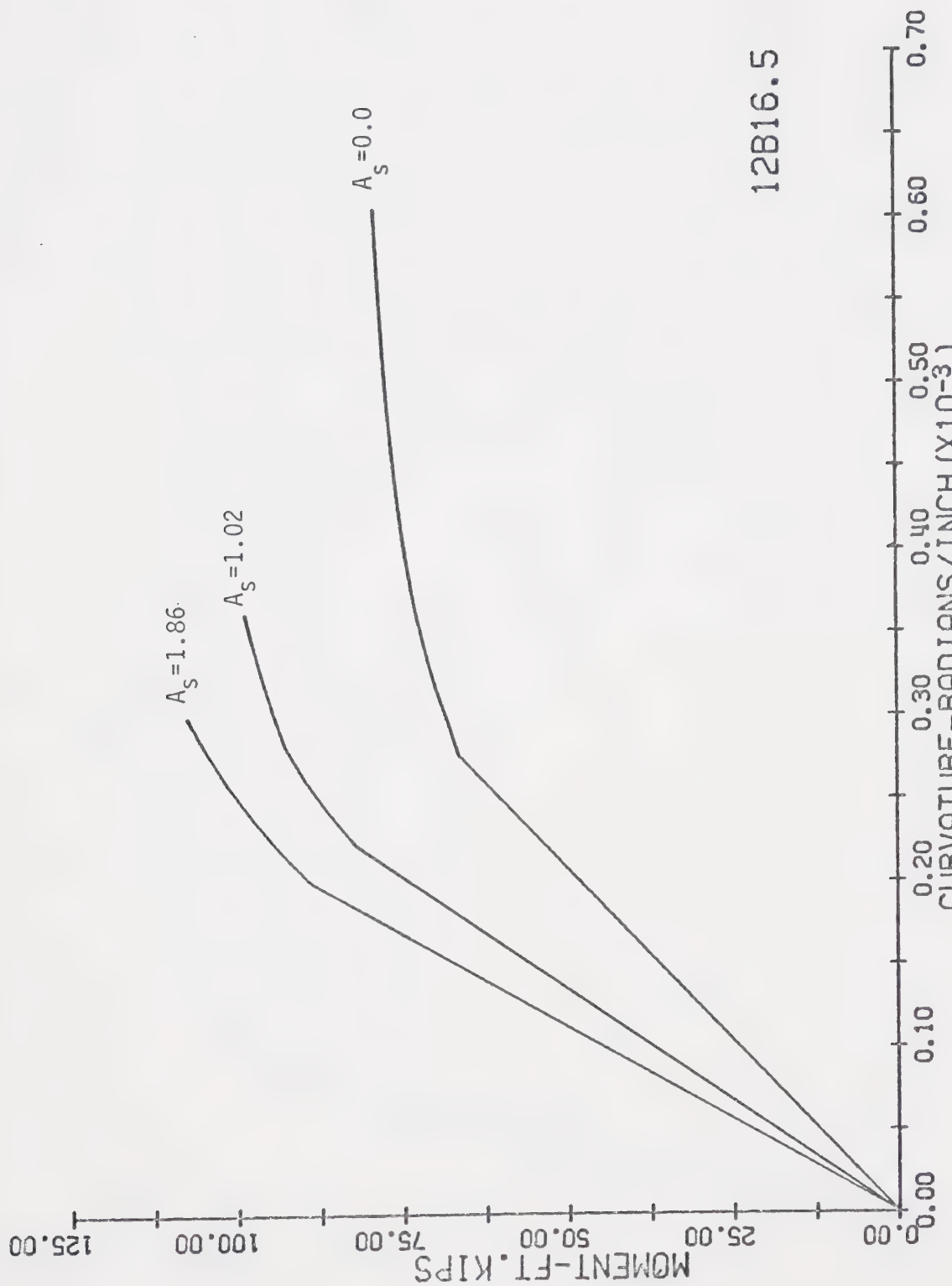

FIGURE 4-6 THEORETICAL MOMENT-CURVATURE DIAGRAM FOR 12B16.5 SERIES
(MODIFIED STRESS-STRAIN DIAGRAM)

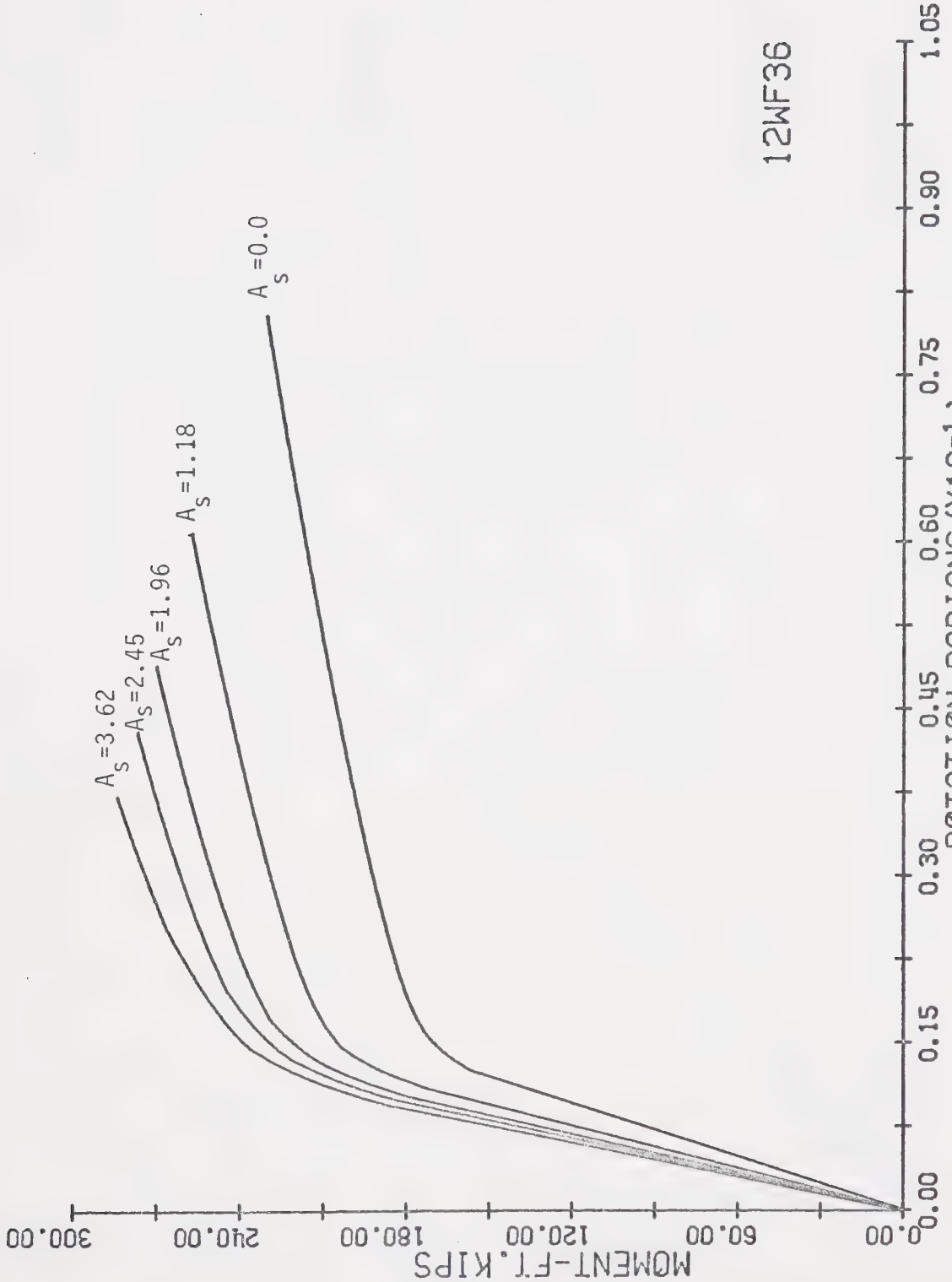

FIGURE 4-7 THEORETICAL MOMENT-ROTATION DIAGRAM FOR 12WF36 SERIES
(MODIFIED STRESS-STRAIN DIAGRAM)

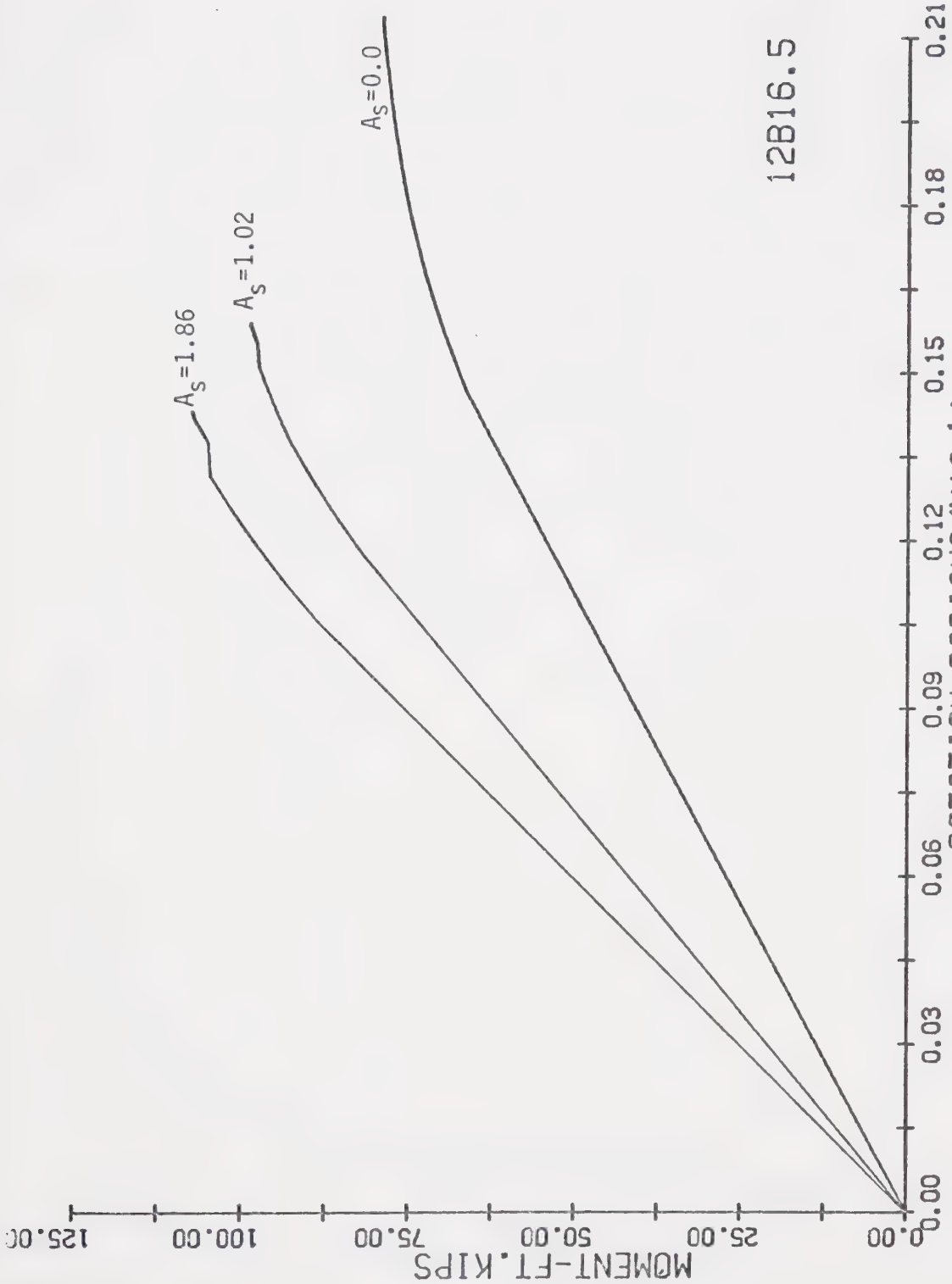

FIGURE 4-8 THEORETICAL MOMENT-ROTATION DIAGRAM FOR 12B16.5 SERIES
(MODIFIED STRESS-STRAIN DIAGRAM)

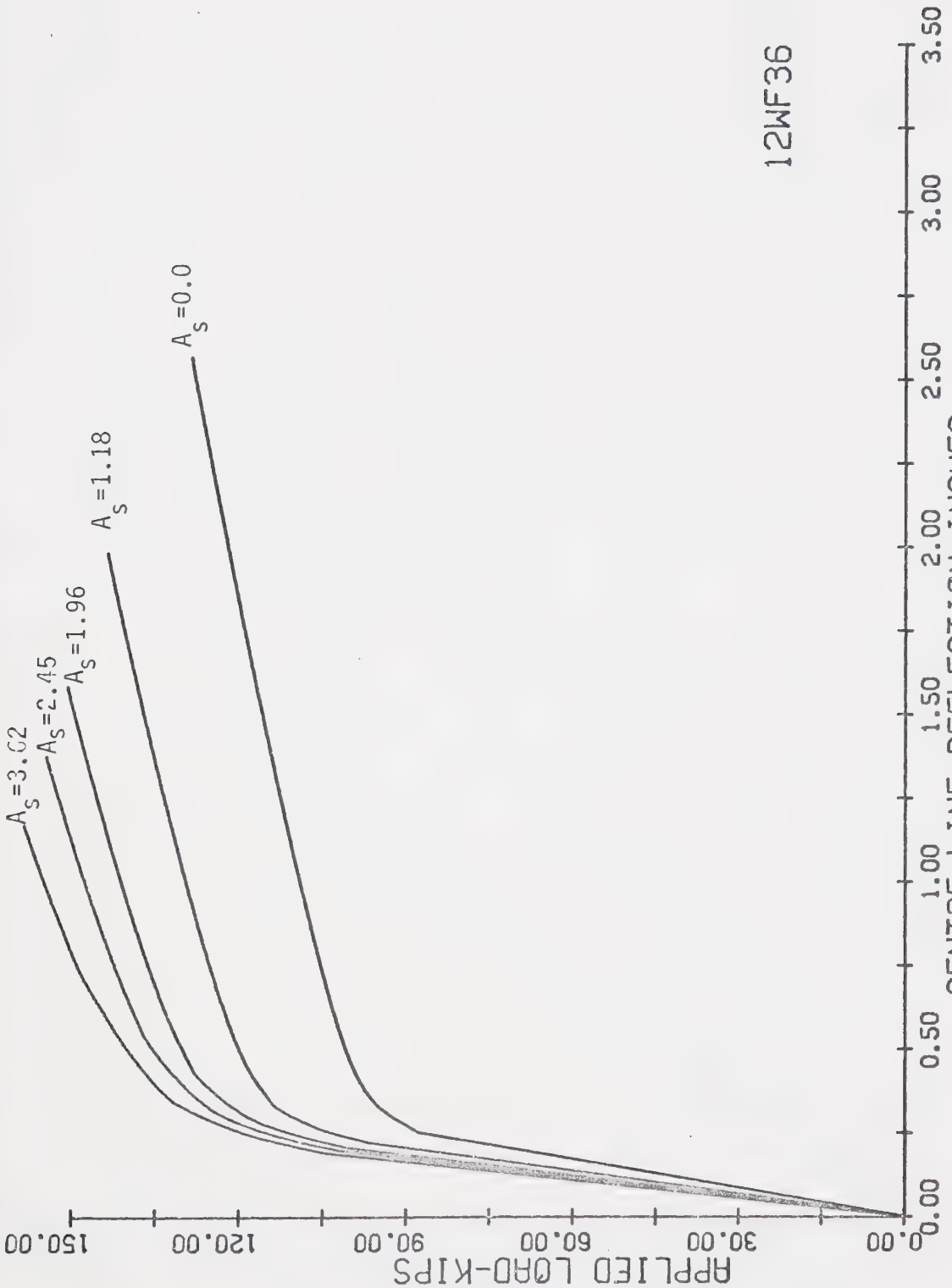

FIGURE 4-9 THEORETICAL LOAD-DEFLECTION DIAGRAM FOR 12WF36 SERIES
(MODIFIED STRESS-STRAIN DIAGRAM)

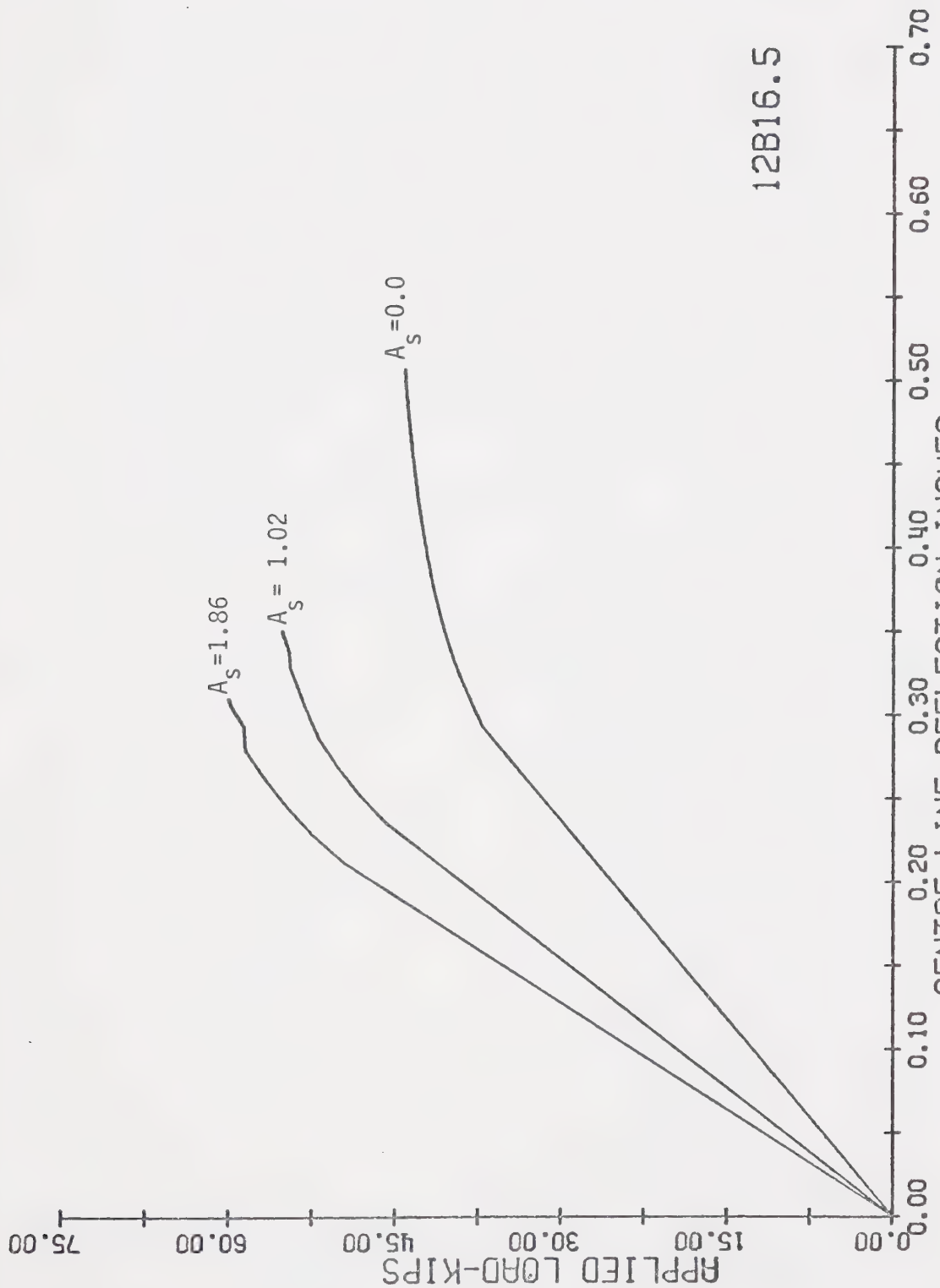

FIGURE 4-10 THEORETICAL LOAD-DEFLECTION DIAGRAM FOR 12B16.5 SERIES
(MODIFIED STRESS-STRAIN DIAGRAM)

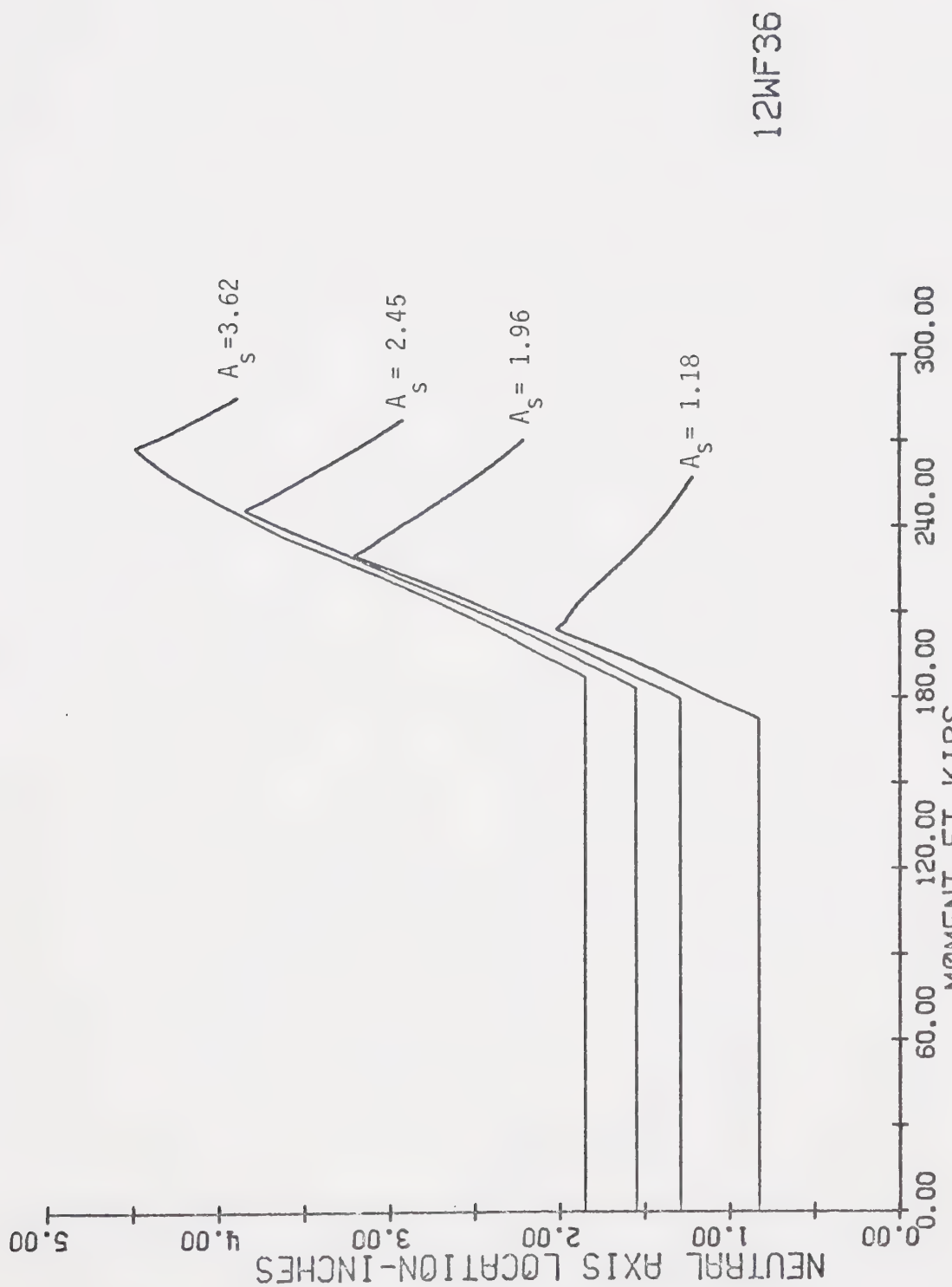

FIGURE 4-11 THEORETICAL MOMENT-NEUTRAL AXIS LOCATION DIAGRAM FOR 12WF36 SERIES
(MODIFIED STRESS-STRAIN DIAGRAM)

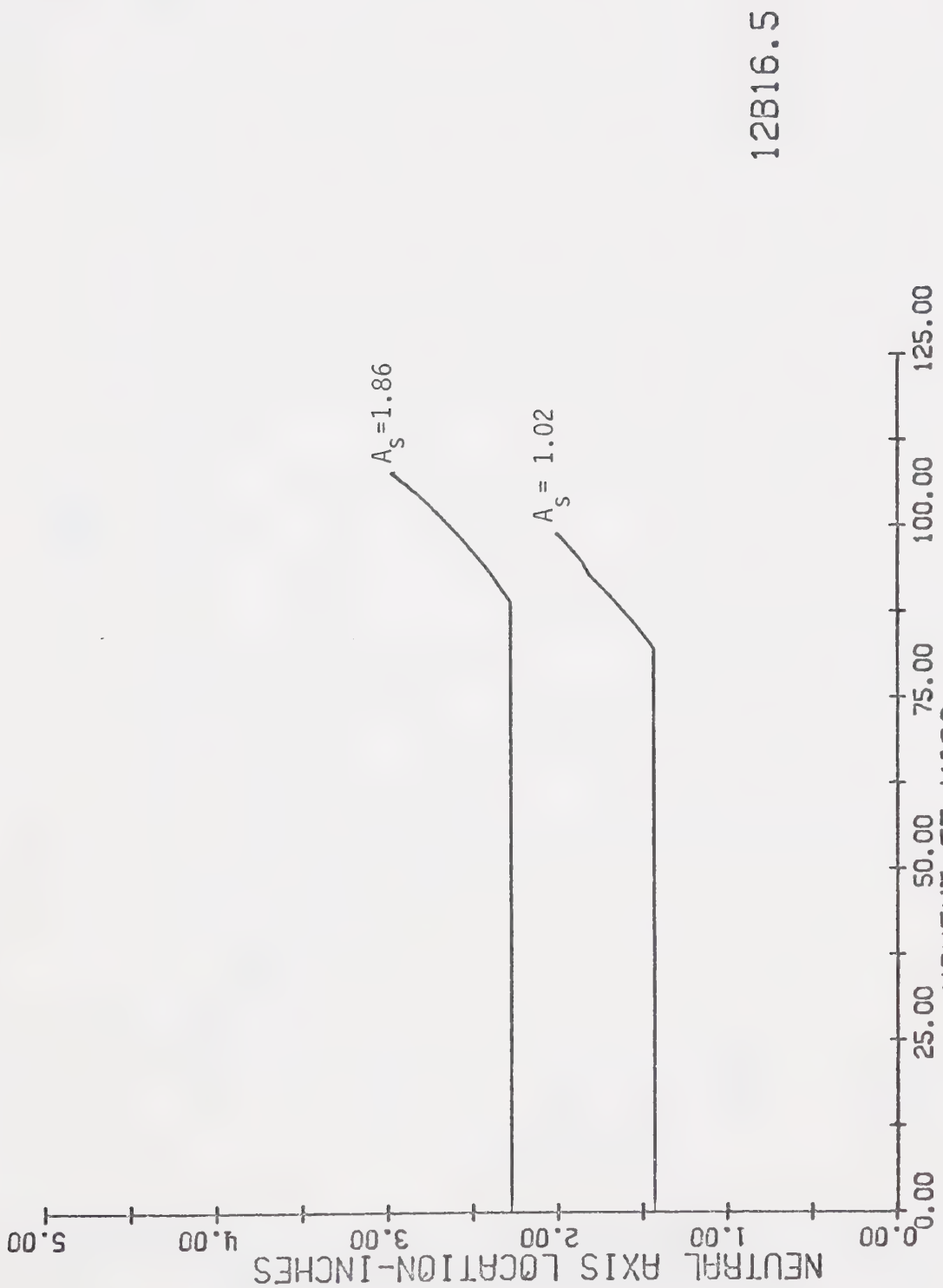

FIGURE 4-12 THEORETICAL MOMENT-NEUTRAL AXIS LOCATION DIAGRAM FOR 12B16.5 SERIES (MODIFIED STRESS-STRAIN DIAGRAM)

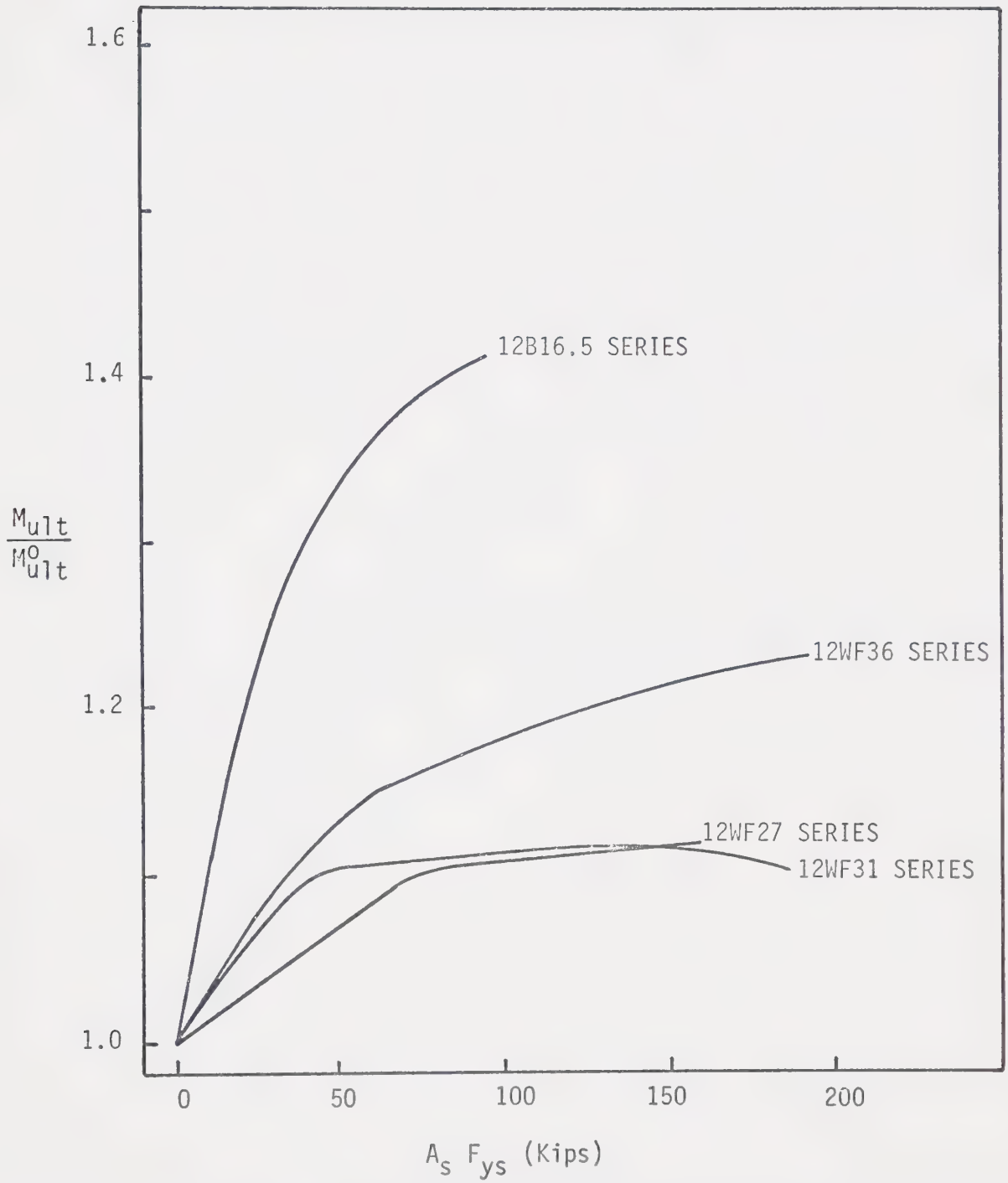

FIGURE 4-13 EXPERIMENTAL RELATIONSHIP BETWEEN MOMENT RATIO M_{ult}/M^o_{ult} AND YIELD FORCE IN SLAB REINFORCEMENT $A_s F_{ys}$

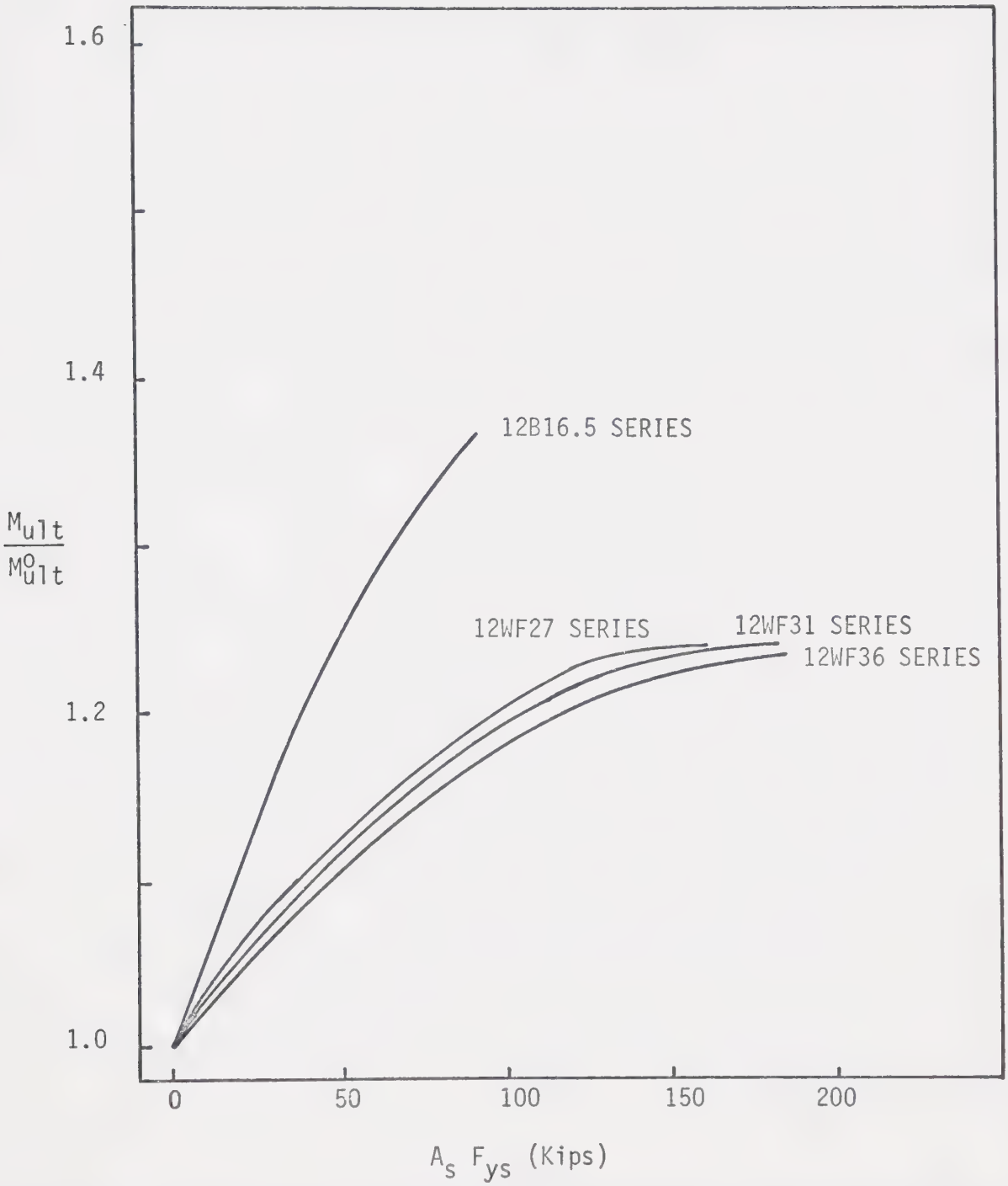

FIGURE 4-14 THEORETICAL RELATIONSHIP BETWEEN MOMENT RATIO M_{ult}/M^o_{ult} AND YIELD FORCE IN SLAB REINFORCEMENT $A_s F_{ys}$

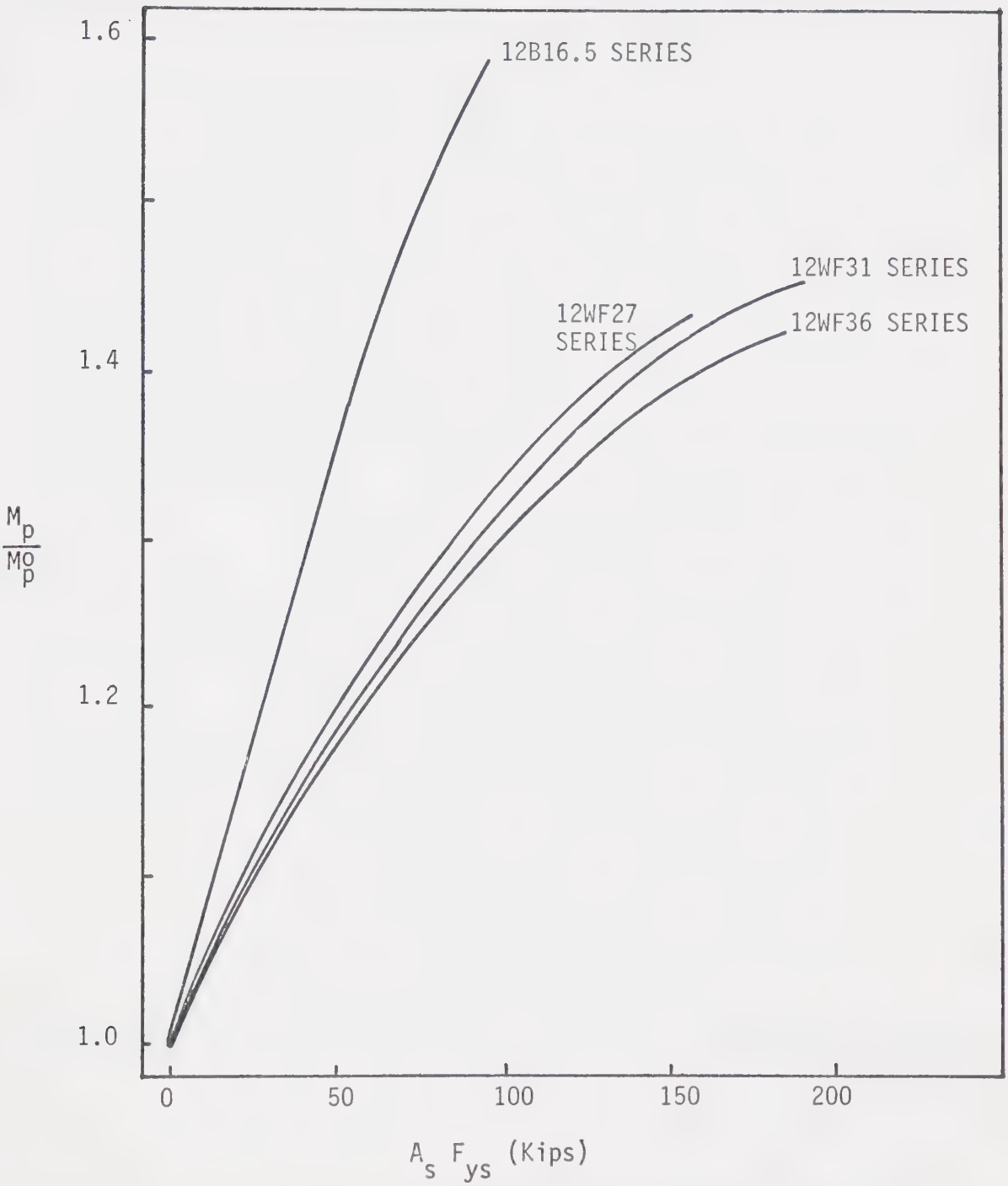

FIGURE 4-15 RELATIONSHIP BETWEEN MOMENT RATIO M_p/M_p^o AND YIELD FORCE IN SLAB REINFORCEMENT $A_s F_{ys}$

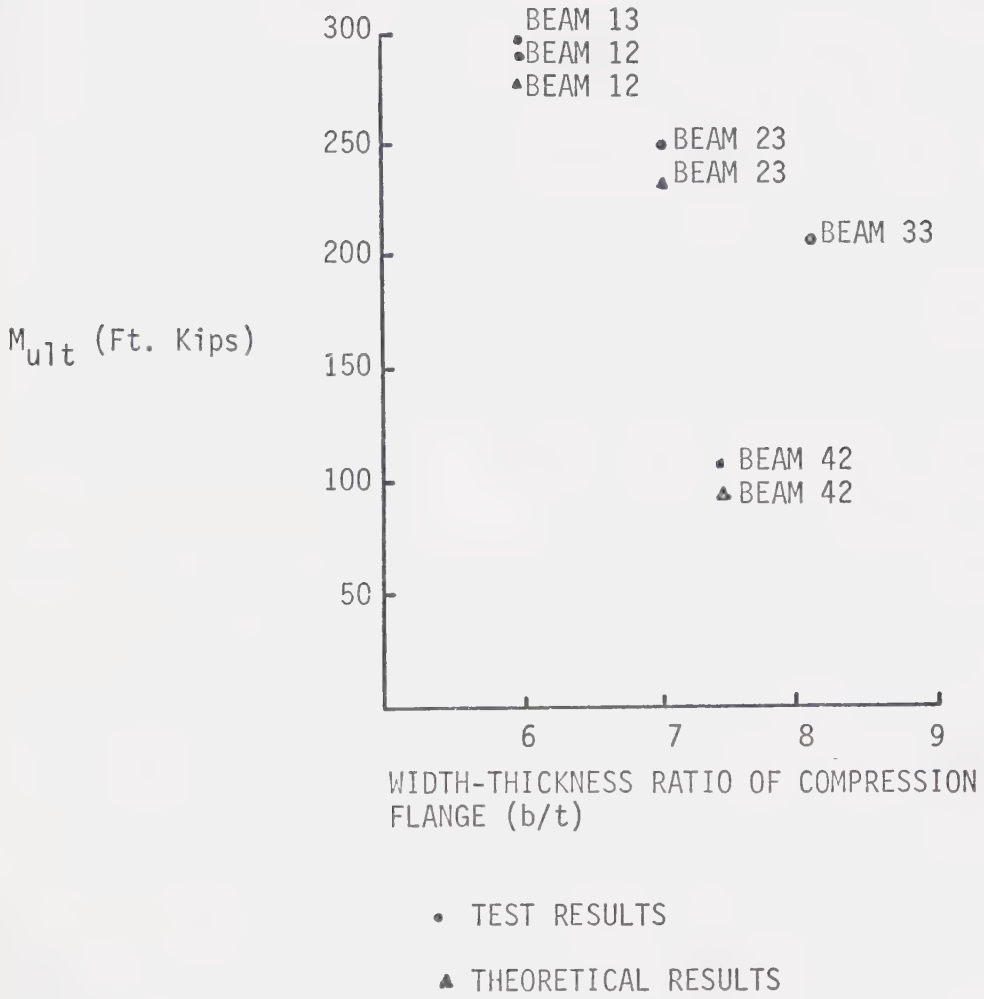

FIGURE 4-16 RELATIONSHIP BETWEEN ULTIMATE MOMENT (M_{ult}) AND b/t RATIO

CHAPTER V

DISCUSSION OF RESULTS

5.1 INTRODUCTION

The following discussion centres on the results of the analyses based on idealized and modified stress-strain disgrams. Comparisons are made between theoretical and experimental results. Factors which may have affected both theoretical and experimental results are discussed.

5.2 COMPARISON OF TWO BASES FOR THEORETICAL SOLUTIONS

The flexural behaviour of a composite member depends on cross-section properties, material properties and the type of loading applied. Material properties may be obtained from a tension test on a coupon of the material. The results of such a test may be defined in the form of an idealized stress-strain diagram. The idealized stress-strain relationship, however, does not satisfactorily define the response of the member to applied load. The presence of residual stresses, in the steel section as a result of the rolling process, is a factor in the resulting stress distribution due to applied moments. The residual stress pattern in the flange varies from compression at the flange tips to tension at the flange-web junction A coupon test does not provide information about residual stresses, since upon cutting the coupon these stresses are released. The

modified stress-strain diagram attempts to approximate the effects of residual stresses.

For the theoretical analysis, material properties such as yield stress, yield strain, strain at strain-hardening and strain-hardening modulus were obtained from coupon tests which were made in connection with the experimental investigations of composite beams at the University of Alberta.

The general flexural behaviour of a composite beam may be defined by moment-curvature relationship. The theoretical moment-curvature relationships (FIGURES 4-3 to 4-6) are very similar in nature to those obtained experimentally (FIGURE 4-1 and 4-2). Use of the modified stress-strain diagram in the analysis results in curves which bear a closer resemblance to the experimental curves than those obtained with the idealized stress-strain diagram. Generally, the modified stress-strain diagram and the idealized stress-strain diagram result in almost identical values of ultimate moment. The curvatures at ultimate, however, are significantly different as the plastic plateau is neglected in the modified stress-strain diagram. The unloading portion of the moment-curvature relationship, subsequent to ultimate moment, is not defined by the theoretical analysis. The effect of increasing the amount of longitudinal slab reinforcement is similar for both experimental and theoretical relationships. Relationships derived from theoretical moment-curvature relations appear in FIGURES 4-7 to 4-12.

In order to fairly assess the validity of the theoretical analysis, one should first examine both the theoretical and

experimental values and decide if any of them are of a questionable nature. TABLE 4.1 indicates that BEAM 25 does not follow the trend of other beams in the same series with respect to ultimate moment value. Therefore, the experimental results for BEAM 25 are suspect. Similarly, the 12WF27 series should probably be excluded from the comparison since the material properties defined by coupon tests appear to be in error. In the 12WF36 series BEAM 18 is inconsistent with respect to the deflection at ultimate moment when compared with other beams of the same series. During testing, BEAM 18 developed a twisting rotation and, therefore, had to be unloaded so shims could be placed under the loading bridge before the load was reapplied. Ultimate deflections rather than ultimate curvatures are compared as it is felt that experimental values of deflections are likely to be more accurate than values of curvatures. At moment values above M_o, strain gauges became inoperative. Therefore, experimental curvatures at moment values above M_o are based on strain gauges located close to the neutral axis.

The theoretical values of ultimate moment differ from experimental values by a maximum of -8% for beams in which the compression flange strain-hardens prior to failure by local buckling. For sections which do not reach strain-hardening of the compression flange, that is, the composite 12B16.5 series, the theoretical ultimate moment value is 12% below the experimental value. For the 12WF31 series, deflections based on the idealized stress-strain diagram are up to 80% greater than the experimental deflections

whereas the values based on the modified stress-strain diagram show a difference from experimental values of -16% to +14%. The 12WF36 series show a maximum difference of -26% between experimental and theoretical ultimate deflections based on the idealized stress-strain diagram. Based on the modified stress-strain diagram the maximum variation is -50%. For the 12B16.5 series, use of the idealized stress-strain diagram results in a 47% difference while the modified stress-strain diagram gives a deflection 53% under the experimental value. The above comparisons indicate that the value of E_{st} or E'_{st} affects the ultimate values of curvature, rotation and deflection to a greater extent than it affects the ultimate moment value. This is also observed in results obtained with E_{st} or E'_{st} varying from E/100 to E/30 or from 3×10^5psi. to 10×10^5psi. From FIGURES 4-3 to 4-6 it is also evident that a small increase in the moment or load value, for values above M_p, results in a significant increase in curvature and related values. Based on theoretical results for the 12WF31 series it appears that the modified stress-strain diagram results in a better agreement between theoretical and experimental values at ultimate moment than does the idealized stress-strain diagram.

On the basis of all the comparisons, the modified stress-strain diagram, therefore, appears to provide the better solution for the flexural behaviour of composite beams in negative bending.

5.3 MATERIAL PROPERTIES

The stress-strain diagrams are derived from values of yield

stress and strain, strain-hardening strains and strain-hardening modulus obtained from tension tests on coupons taken from the beams tested in the experimental investigations. As TABLE 4.6 shows, a wide variation can exist in the above values obtained from coupons taken from the section. It is, therefore, questionable whether average values obtained from coupon tests are likely to be more valid than standard values specified for the given material, in this case G40.12 steel. The strain-hardening modulus, in particular, appears to vary considerably. Other investigators indicate that the strain-hardening modulus may vary between E/100 and E/30, in other words from 3×10^5psi. to 10×10^5psi.

Theoretical results based on standard material properties for CSA G40.12 steel (F_y = 44 ksi, E = 29000 ksi) with E_{st} and E'_{st} ranging from E/100 to E/30 were obtained. The results indicate that, as E_{st} is increased, ultimate deflections decrease whereas the moment at ultimate remains fairly constant. Compared with experimental results, the moment at ultimate is over estimated by a maximum of 15% while the deflections at ultimate represent upper and lower limits to the experimental values. Based on the above, it appears that standard values may be used to determine the flexural behaviour of composite beams in negative bending.

5.4 NEUTRAL AXIS LOCATION

FIGURES 4-11 and 4-12 indicate the initial tendency of the neutral axis to move towards the tension flange with increasing moment and increasing longitudinal slab reinforcement. Initially the neutral

axis is located at the centroid of the composite section. Its location is constant until the moment reaches the value M_o. Once yielding begins, the neutral axis moves towards the tension flange with increasing moment. This movement is halted either by strain-hardening of the compression flange or yielding of the longitudinal slab reinforcement. The latter is more likely to happen before the former. As moment increases still further, the neutral axis moves towards the compression flange. For the 12B16.5 series, which do not exhibit evidence of strain-hardening, there is no tendency for the neutral axis location to shift towards the compression flange at moment values above M_o.

5.5 ULTIMATE LOAD CONDITIONS

Values in TABLES 4.1, 4.2 and 4.3 have been used in several plots to show the effects of longitudinal slab reinforcement and size of the steel section on the ultimate moment capacity. In FIGURE 4-14, for the 12B16.5 series it is evident that an increase in the amount of longitudinal slab reinforcement results in a substantial increase in the M_{ult}/M^o_{ult} ratio. The other series, however, exhibit a more gradual increase in M_{ult}/M^o_{ult} for low amounts of longitudinal slab reinforcement. Above the limit of reinforcement which places the neutral axis into the tension flange, the increase in M_{ult}/M^o_{ult} is 1% or less as the area of reinforcement is reduced to the upper limit value given by EQUATION (3-1). The increase in the experimental M_{ult}/M^o_{ult} ratio is less than 2%. The increase in the M_{ult}/M^o_{ult} ratio is not as great as the increase in the M_p/M^o_p ratio for the series involving wide flange sections. The increase in ultimate moment is,

therefore, not directly proportional to the increase in the simple plastic moment (as shown in FIGURE 4-15). FIGURE 4-13 shows the experimental results for comparison.

FIGURE 4.16 indicates that the theoretical moment capacity is dependent on the b/t ratio of the steel section. For composite sections with similar A_s/A_{WF} ratios, where the compression flange strain-hardened prior to ultimate moment conditions, an almost linear relationship exists between the b/t ratio and the ultimate moment. This relationship is verified by the experimental results. BEAM 42 does not follow this trend since local buckling occurs prior to strain-hardening of the compression flange.

CHAPTER VI

CONCLUSIONS

From a comparison of theoretical and experimental results it is concluded that:

1) The ultimate moment capacity of a composite section in negative bending may be computed by the proposed theory. Theoretical values of ultimate moment, based on actual material properties as obtained for test specimens at the University of Alberta, are a maximum of 8% below experimental values for the beams failing after strain-hardening of the compression flange. For section failing prior to strain-hardening of the compression flange, the theoretical ultimate moment is 12% below experimental values.

2) Use of a modified stress-strain diagram consisting of an elastic range and a strain-hardening range produces results closer to test results than those obtained using an idealized stress-strain diagram consisting of elastic, plastic and strain-hardening ranges.

3) The upper limit on the effective area of longitudinal slab reinforcement can be satisfactorily determined on the basis of a neutral axis location, for the plastic moment value, at the inner face of the tension flange.

4) Ultimate moment values are not particularly sensitive

to the value of the strain-hardening modulus, but curvatures, deflections and rotations are very sensitive. Theoretical results obtained using the modified stress-strain diagram with the strain-hardening modulus varying from E/100 to E/30 result in a relatively small increase (less than 1%) in the ultimate moment whereas corresponding curvatures decreased from an upper limit for the experimental values to a lower limit.

The theoretical analysis verifies the following conclusions established in experimental investigations by Lever (3) and Davison (2):

1) For a given steel section, significant increases in the ultimate capacity of composite beams in negative bending can be achieved by the addition of longitudinal slab reinforcement.

2) The increase in the ultimate moment capacity is not directly proportional to the increase in the simple plastic moment value.

3) For a given steel section, an increase in the amount of longitudinal slab reinforcement results in a reduction in the rotation capacity of a negative plastic hinge.

REFERENCES

1. Piepgrass, E. B., "Behaviour of Composite Beams in Negative Bending", Masters Thesis, Department of Civil Engineering, University of Alberta, June 1968.

2. Davison, J. H., "Composite Beams in Negative Bending", Masters Thesis, Department of Civil Engineering, University of Alberta, May 1969.

3. Lever, G. V., "Ultimate Strength of Composite Beams in Negative Bending", Masters Thesis, Department of Civil Engineering, University of Alberta, Spring 1970.

4. Bleich, F., "Buckling Strength of Metal Structures", McGraw-Hill Book Company Inc., New York, N.Y., 1952.

5. Haaijer, G., "Plate Buckling in the Strain-Hardening Range", Journal of the Engineering Mechanics Division, Proc. A.S.C.E., Vol. 83, No. EM2, April 1957, p. 1212-1.

6. Lay, M. G., "Flange Local Buckling in Wide Flange Shapes", Journal of the Structural Division, Proc. A.S.C.E., Vol. 91, No. ST6, December 1965, p. 95.

7. Lay, M. G., and Galambos, T. V., "Inelastic Beams Under Moment Gradient", Journal of the Structural Division, Proc. A.S.C.E., Vol. 93, No. ST1, February 1967, p. 381.

8. Canadian Standards Association Standard S16 - 1969, "Steel Structures for Buildings", December 1969.

APPENDIX A

COMPUTER PROGRAM

A.1 COMPUTER PROGRAM

The computer program, written in FORTRAN IV language for the IBM 360/67 system, calculates and plots moment-curvature, moment-total rotation and load-deflection relationships and determines the location of the neutral axis for composite sections in negative bending. The calculations follow the procedure described in CHAPTER III.

Subroutines are used to calculate the centroid of the section and the moment of inertia about the x-axis, to list most of the calculated values and to plot the calculated relationships. The flow chart for the main program is given in APPENDIX A.3 and some of the notation used is described in APPENDIX A.2. The formulation of the subroutines can be followed in the program listing presented in APPENDIX A.4.

A.2 NOTATION USED IN COMPUTER PROGRAM

SECT, D, B, TT, WW, H	- steel section and physical properties of steel section
TITLE	- brief description of input
TYW, TYF, TYS	- yield stresses of web, flange and longitudinal slab reinforcement
EF, EW, ER	- Young's modulus for flange, web and longitudinal slab reinforcement
ESTF, ESTW, ESTR	- strain hardening modulus for flange, web and longitudinal slab reinforcement
STRYF, STRYW, STRYR	- yield strain of flange, web and slab reinforcement
STSTF, STSTW, STSTR	- strain hardening strains of flange, web and slab reinforcement
LPLOT	- determines scale to which plots are drawn in Subroutine GRAPH
FACTOR	- amount of slip considered to occur between slab and steel section
DIST	- distance between reaction and load point
XDIST	- length of beam, this is divided by 2 and value obtained is also designated as XDIST
GE	- elastic shear modulus
U	- Poisson's ratio

AF, AW	- ratio of Young's modulus to strain hardening modulus for flange and web
GTF, GTW	- inelastic shear moduli of flange and web
WI	- variable used in calculating length of flange required to yield for formation of local buckle
ICHECK	- integer counter
AREA 1, AREA 2, AREA 3, AREA 4, AREA 5	- variables used in calculating rotation and deflection of beam
FS, FF, FW	- forces in reinforcement, flange and web used in computing simple plastic moment
NA	- neutral axis location, above compression flange, for simple plastic moment
Y	- depth of top flange in compression
MS, MTF, MBF, MW	- contributions to plastic moment of reinforcement, top flange, bottom flange and web
MP	- simple plastic moment
Z	- assumed distance between neutral axis and compression flange
INCR	- value by which neutral axis is shifted if assumed location of neutral axis does not result in

	equilibrium of section
ECF, ECW	- compressive strains in web and flange
ETW, ETF, EAS	- tensile strains in web, flange and reinforcement
ELAST	- elastic portion of web in compression
ZZ	- depth of compression zone of web which is inelastic
FCW, FCYW, FCEW	- forces in web in compression
FCF	- force in compression flange
FTW, FTYW, FTEW	- forces in tensile portion of web
FTF	- force in tension flange
FAS	- tensile force in reinforcement
SUMF	- sum of forces in section
N	- integer counter
MUAS, MUTF, MUTW, MUTYW, MUTEW, MUCEW, MUCYW, MUCW, MUCF	- contributions to moment in section due to specified curvature
MULT	- total resisting moment of section
AMPS	- moment at first yield of compression flange
APHI	- curvature at first yield of compression flange
XOPT	- distance required for local buckle to form
XMPS	- ultimate moment (moment at which local buckling of compression flange

	occurs)
SK	- torsional spring constant
ADIST	- distance between neutral axis and centroid of steel section
PINCR	- amount by which curvature is increased
JJ, KJ	- integer counters
SRATIO	- inelastic portion of beam
BMTOT (JJ), BPHI (KJ), ROT (JJ), ALOAD (JJ), DELTA (JJ), ADIST (JJ)	- related values, at any loading, of moment, curvature, rotation, load, deflection and distance between neutral axis and centroid of steel section
PHI, UNIT	- curvature of section at a specified load
XRATIO	- elastic length of beam
AIX	- moment of inertia of section considered
YBAR	- centroid of section considered
NNKK	- integer counter

A.3 FLOWCHART FOR MAIN PROGRAM

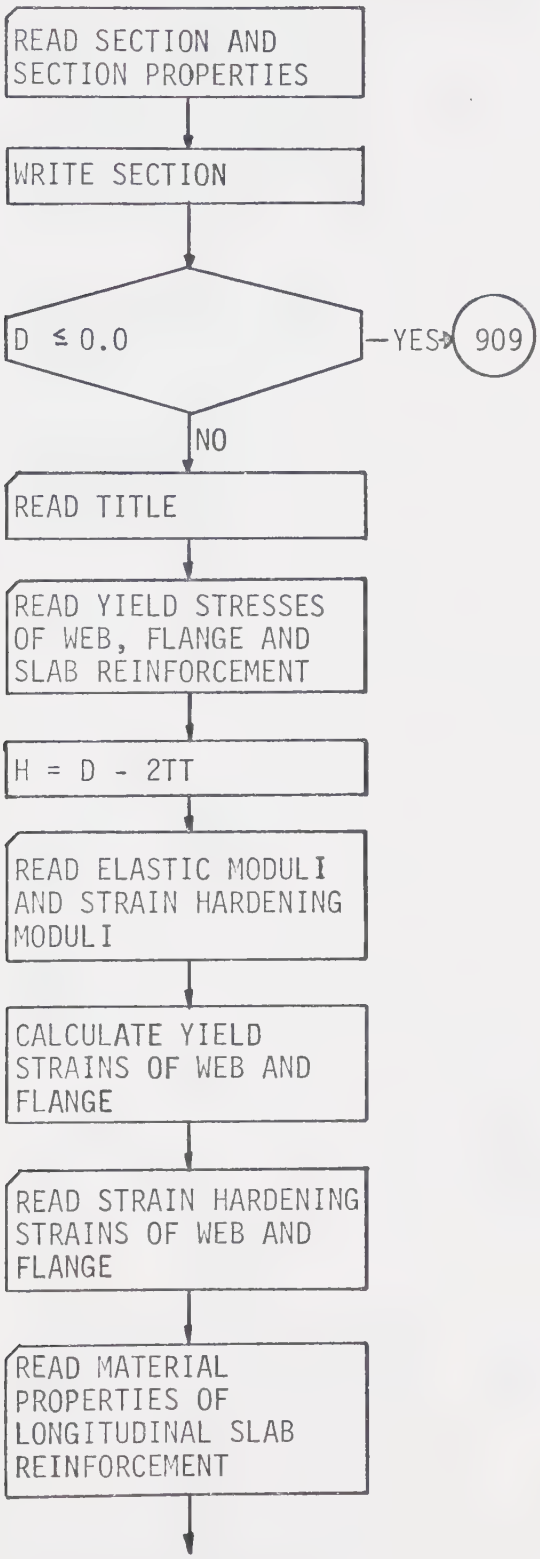

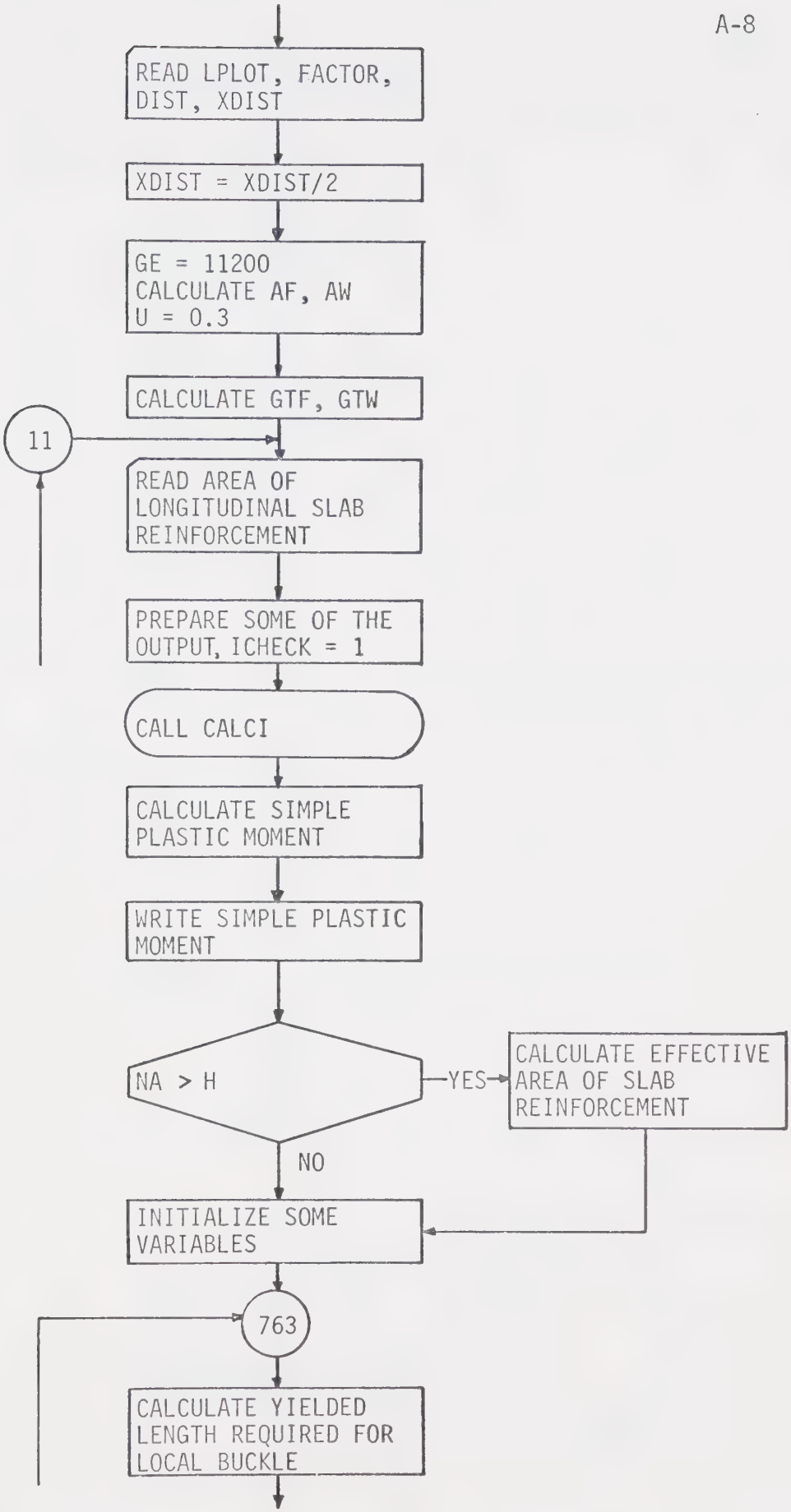
READ LPLOT, FACTOR, DIST, XDIST
XDIST = XDIST/2
GE = 11200
CALCULATE AF, AW
U = 0.3
CALCULATE GTF, GTW
11
READ AREA OF LONGITUDINAL SLAB REINFORCEMENT
PREPARE SOME OF THE OUTPUT, ICHECK = 1
CALL CALCI
CALCULATE SIMPLE PLASTIC MOMENT
WRITE SIMPLE PLASTIC MOMENT
NA > H
YES
CALCULATE EFFECTIVE AREA OF SLAB REINFORCEMENT
NO
INITIALIZE SOME VARIABLES
763
CALCULATE YIELDED LENGTH REQUIRED FOR LOCAL BUCKLE

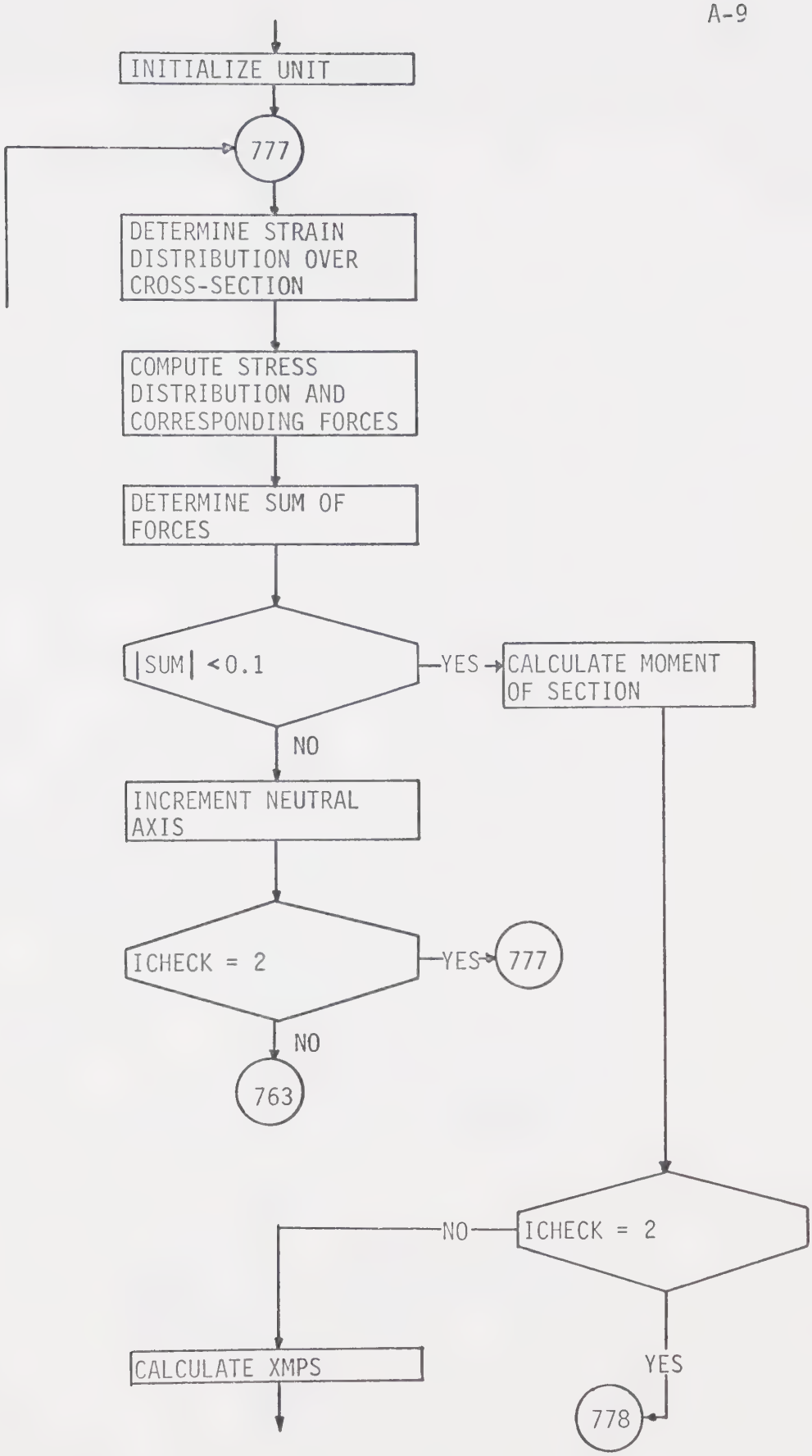
INITIALIZE UNIT
777
DETERMINE STRAIN DISTRIBUTION OVER CROSS-SECTION
COMPUTE STRESS DISTRIBUTION AND CORRESPONDING FORCES
DETERMINE SUM OF FORCES
|SUM| <0.1
YES
CALCULATE MOMENT OF SECTION
NO
INCREMENT NEUTRAL AXIS
ICHECK = 2
YES
777
NO
763
ICHECK = 2
NO
CALCULATE XMPS
YES
778

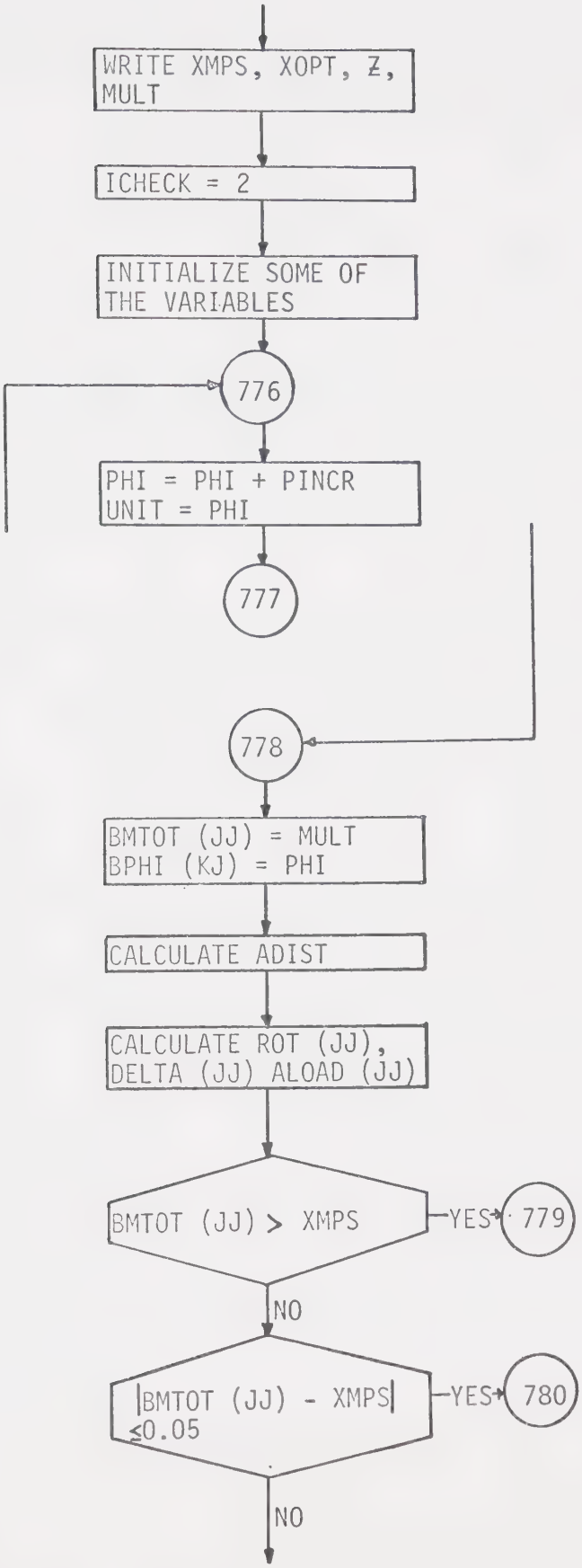
WRITE XMPS, XOPT, Z, MULT
ICHECK = 2
INITIALIZE SOME OF THE VARIABLES
776
PHI = PHI + PINCR
UNIT = PHI
777
778
BMTOT (JJ) = MULT
BPHI (KJ) = PHI
CALCULATE ADIST
CALCULATE ROT (JJ), DELTA (JJ) ALOAD (JJ)
BMTOT (JJ) > XMPS
YES
779
NO
|BMTOT (JJ) - XMPS| ≤0.05
YES
780
NO

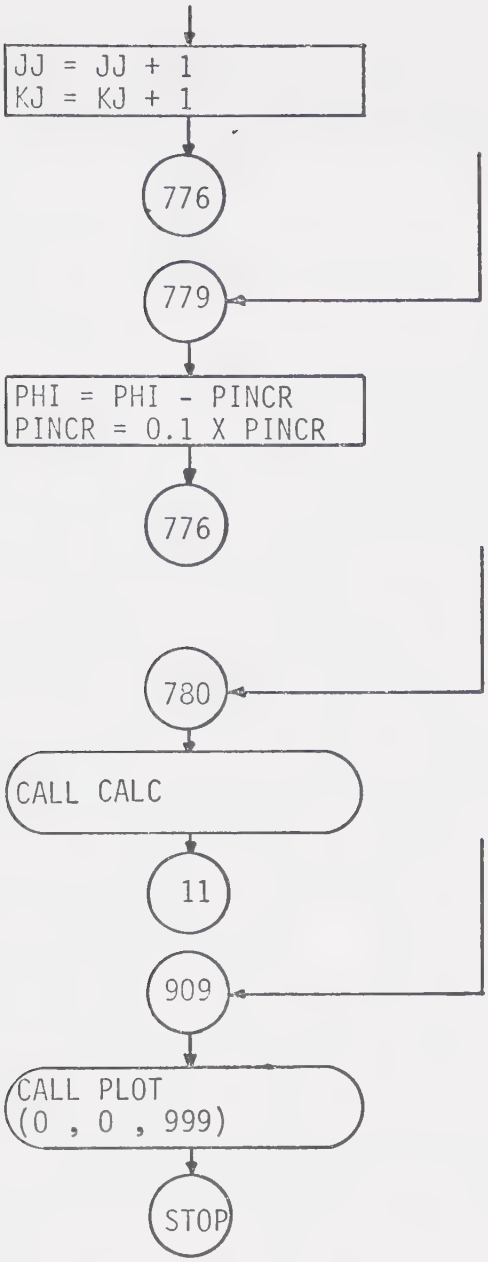
JJ = JJ + 1
KJ = KJ + 1
776
779
PHI = PHI - PINCR
PINCR = 0.1 X PINCR
776
780
CALL CALC
11
909
CALL PLOT
(0 , 0 , 999)
STOP

A.4 PROGRAM LISTING

```
      DIMENSION DATA(1024)
      DIMENSION SRATIO(4000)
      COMMON ROT(4000)
      COMMON JPLOT,LPAGE,TITLE(20),LPLOT,SECT(10),XMPS,ADIST(4000)
      COMMON A(10),T(10),W(10),E(10),ESH(10),S(10),SSH(10),BMTOT(4000)
      COMMON BPHI(4000),JJ,KJ,ALOAD(4000),DELTA(4000),AIX
      REAL MUTF,MUTYW,MUAS,MUTW,MUCF,MUCYW,MUCW,MULT ,INCR,MUCEW,MUTEW
      REAL MS,MTF,MBF,MW,MP,MTFT,MTFC,MWT,MWC,NA
      CALL PLOTS (DATA(1),4096)
      JPLOT=1
C     **
C     ** READ IN SECTION AND SECTION PROPERTIES
C     **
C     **
C     ** D=DEPTH OF X-SECTION, B=WIDTH OF FLANGE,TT= THICKNESS OF FLANGE,
C      ** WW= THICKNESS OF WEB
C     ** DD EQUALS DISTANCE THAT REINF. OF SLAB IS ABOVE TENSION FLANGE
C     **
C     **
    1 READ(5,100) (SECT(I),I=1,2),D,B,TT,WW,DD
  100 FORMAT(2X,2A4,5F10.6)
      WRITE(6,200)(SECT(I),I=1,2)
  200 FORMAT(1H1,10X,'SECTION IS ',2A4,//)
      IF(D.LE.0.0)GO TO 909
      READ(5,623)(TITLE(I),I=1,20)
  623 FORMAT(20A4)
      WRITE(6,624)(TITLE(I),I=1,20)
  624 FORMAT(12X,20A4,//)
C     **
C     ** READ IN YIELD STRESSES OF WEB,FLANGE AND REINFORCEMENT
C     ** TYW = YIELD STRESS OF WEB, TYF = YIELD STRESS OF FLANGE,
C     ** TYS = YIELD STRESS OF REINFORCEMENT STEEL  ******
C     **
      READ(5,300)TYW,TYF,TYS
  300 FORMAT(3F10.6)
      H=D-(2.*TT)
C     **
C     ** READ IN ELASTIC MODULUS AND STRAIN HARDENING MODULUS
C     **
      READ(5,500) EF,EW,ESTF,ESTW
  500 FORMAT(4F20.6)
C     **
C     ** CALCULATE YIELD STRAINS OF WEB AND FLANGE.
C     **
      STRYF=TYF/EF
      STRYW=TYW/EW
C     **
C     **  READ IN STRAIN HARDENING STRAINS
```

```
C      **
       READ(5,4000)STSTF,STSTW
 4000 FORMAT(2F20.10)
C
C      READ IN MATERIAL PROPERTIES FOR SLAB STEEL
C
       READ(5,4002)ER,ESTR,STSTR
 4002 FORMAT(3F20.10)
       STRYR=TYS/ER
C
C      LPLOT DETERMINES THE SCALE TO WHICH THE MOMENT ROTATION CURVES ARE DRAWN
C       FACTOR EQUALS SLIP BETWEEN REINF.AND STEEL SECTION
C      DIST EQUALS DISTANCE BETW. REACTION POINT AND LOAD POINT
C
       READ(5,4001)LPLOT,FACTOR,DIST,XDIST
 4001 FORMAT(I2,3F10.5)
       XDIST=XDIST/2.
       GE=11200.
C      **
C      **
C      ** AF = RATIO OF ELASTIC MODULUS OF FLG TO STRAIN HARDENING MODULUS
C      ** AW = RATIO OF ELASTIC MODULUS OF WEB TO STRAIN HARDENING MODULUS
C      **
C      **
       AF=EF/ESTF
       AW=EW/ESTW
C      **
C      ** U = POISSONS RATIO
C      **
       U=.3
C      **
C      **
C      ** GTW, GTF ARE INELASTIC SHEAR MODULI
C      **
C      **
       GTW=(2.*GE)/(1.+AW/(4.*(1.+U)))
       GTF=(2.*GE)/(1.+AF/(4.*(1.+U)))
       WI=(((E**3)*TT**3)*7.)/(16.*144.)
C      **
C      ** READ IN AREA OF REINFORCEMENT
C      **
   11  READ(5,400)AS
 400   FORMAT(F10.6)
       AREA1=0.
       AREA2=0.
       AREA3=0.
       AREA4=0.
       AREA5=0.
       ICHECK=1
       IF(AS.GT.10.0) GO TO 1
       DO 800 K=1,5
       IF(K.EQ.1)GO TO 801
       IF(K.EQ.2)GO TO 802
       IF(K.EQ.3)GO TO 803
       IF(K.EQ.4)GO TO 802
       IF(K.EQ.5)GO TO 804
  801  CONTINUE
       A(K)=AS
       T(K)=DD*2.
       W(K)=2.
```

```
      E(K)=ER
      ESH(K)=ESTR
      S(K)=STRYR
      SSH(K)=STSTR
      GO TO 805
  802 CONTINUE
      A(K)=B*TT
      T(K)=TT
      W(K)=B
      E(K)=EF
      ESH(K)=ESTF
      S(K)=STRYF
      SSH(K)=STSTF
      GO TO 805
  803 CONTINUE
      A(K)=H*WW
      T(K)=H
      W(K)=WW
      E(K)=EW
      ESH(K)=ESTW
      S(K)=STRYW
      SSH(K)=STSTW
      GO TO 805
  804 CONTINUE
      A(K)=0.
      T(K)=0.
      W(K)=0.
      E(K)=0.
      ESH(K)=0.
      S(K)=0.
      SSH(K)=0.
  805 CONTINUE
  800 CONTINUE
      WRITE(6,919)
  919 FORMAT(10X,'-------------------------------------------------')
      CALL CALCI
      WRITE(6,600)AS
  600 FORMAT(10X,'  AREA OF REINFORCEMENT IS  ',F5.2,' SQUARE INCHES',/)
C     **
C     ** COMPUTE PLASTIC MOMENT **
C     **
      FS=AS*TYS
      FF=TYF*B*TT
      FW=TYW*H*WW
      IF(FS.GT.FW) GO TO 2
      IF(FS.LT.FW) GO TO 3
      MS=FS*(TT+DD)
      MTF=FF*(TT/2.)
      MBF=FF*(H+TT/2.)
      MW=FW*(H/2.)
      MP=(MS+MTF+MBF+MW)/12.
      NA=H
      GO TO 4
    2 CONTINUE
      F=(FW+(2.*FF)-FS)/2.
      Y=(F)/(TYF*B)
      FFTC=FF-F
      MS=FS*(DD+Y)
      MTFT=F*(Y/2.)
      MTFC=FFTC*((TT-Y)/2.)
```

```
      MW=FW*(H/2.+(TT-Y))
      MBF=FF*(H+((TT/2.)+(TT-Y)))
      MP=(MS+MTFT+MTFC+MW+MBF)/12.
      NA=H+(TT-Y)
      GO TO 4
    3 CONTINUE
      F=(FW-FS)/2.
      Y=(F)/(TYW*WW)
      FWC=FW-F
      MS=FS*(Y+TT+DD)
      MTF=FF*(Y+(TT/2.))
      MBF=FF*(H-Y+(TT/2.))
      MWT=F*(Y/2.)
      MWC=FWC*((H-Y)/2.)
      MP=(MS+MTF+MBF+MWT+MWC)/12.
      NA=H-Y
    4 CONTINUE
      WRITE(6,501)MP
  501 FORMAT(12X,'PLASTIC MOMENT OF SECTION IS ', F8.3,'FT.K.')
      WRITE(6,700)NA
  700 FORMAT(12X,'NEUTRAL AXIS LOCATION IS ' ,F7.3,' INCHES ABOVE COMPRE
     1SSION FLANGE',/)
      IF(NA.GT.H)AS=FW/TYS
      WRITE(6,297)AS
  297 FORMAT(12X,'AREA OF STEEL REQUIRED IS  ',F6.3,' SQ.IN.')
      Z=NA-1.
      IF(AS.EQ.0.0)Z=H/2.
      INCR=.2
      ELIST=0.
      SUM=0.
      N=0
  763 CONTINUE
      SK=(GTF*WW**3)/(3.*Z)
      XL=3.14159*SQRT(SQRT(ESTF*WI/SK))
      XCRT=2.*XL
      UNIT=STRYF/(Z+TT/2.)
  777 CONTINUE
      ELAST=STRYW/UNIT
C
C     DETERMINE STRAIN DISTRIBUTION OVER X-SECTION
C
      ECF=UNIT*(Z+TT/2.)
      ECW=UNIT*Z
      ETW=UNIT*(H-Z)
      ETF=UNIT*(H-Z+(TT/2.))
      EAS=UNIT*(H-Z+TT+DD)*FACTOR
      IF(ECW.LE.STSTW)GO TO 60
C
C     ZZ = DEPTH OF COMPRESSION ZONE OF WEB WHICH IS PLASTIC
C     Z = DEPTH OF WEB IN COMPRESSION
C     ELAST = ELASTIC REGION OF WEB
C     CONSIDER COMPRESSION ZONE OF WEB
C
      ZZ=((STSTW-STRYW)*(Z-ELAST))/(ECW-STRYW)
      TCW=(ECW-STSTW)*ESTW
      FCW=(TCW*WW*(Z-ZZ-ELAST))/2.
      GO TO 61
   60 CONTINUE
      IF(ECW.LE.STRYW)GO TO 601
      TCW=0.
```

```
      FCW=0.
   61 CONTINUE
      FCYW=TYW*WW*(Z-ELAST)
      FCEW=(TYW*WW*ELAST)/2.
      GO TO 602
  601 CONTINUE
      ELAST=Z*1.
      FCW=0.
      FCYW=0.
      FCEW=(ECW*EW*Z*WW)/2.
  602 CONTINUE
C
C     CONSIDER COMPRESSION FLANGE
C
      IF(ECF.LE.STRYF)GO TO 92
      IF(ECF.LE.STSTF)GO TO 62
      TCF=(ECF-STSTF)*ESTF+TYF
      FCF=TCF*B*TT
      GO TO 63
   62 CONTINUE
      FCF=TYF*B*TT
      GO TO 63
   92 CONTINUE
      FCF=B*TT*ECF*EF
   63 CONTINUE
C
C     CONSIDER PORTION OF WEB IN TENSION
C
      IF(ETW.LE.STSTW)GO TO 64
      TTW=(ETW-STSTW)*ESTW
      FTW=(TTW*WW*(H-Z-ZZ-ELAST))/2.
      GO TO 65
   64 CONTINUE
      IF(ETW.LE.STRYW)GO TO 641
      FTW=0.
   65 CONTINUE
      FTYW=TYW*WW*(H-Z-ELAST)
      FTEW=(TYW*WW*ELAST)/2.
      GO TO 642
  641 CONTINUE
      ELIST=H-Z
      FTW=0.
      FTYW=0.
      FTEW=(ETW*WW*EW*ELIST)/2.
  642 CONTINUE
C
C     CONSIDER FLANGE IN TENSION
C
      IF(ETF.LE.STRYF)GO TO 93
      IF(ETF.LE.STSTF)GO TO 66
      TTF=((ETF-STSTF)*ESTF)+TYF
      FTF=TTF*B*TT
      GO TO 67
   66 CONTINUE
      FTF=TYF*B*TT
      GO TO 67
   93 CONTINUE
      FTF=B*TT*ETF*EF
   67 CONTINUE
```

```
C       CONSIDER SLAB REINFORCEMENT
C
        IF(EAS.LE.STRYR)GO TO 68
        FAS=TYS*AS
        GO TO 69
   68   CONTINUE
        TAS=EAS*ER
        FAS=TAS*AS
   69   CONTINUE
C
C       TEST FOR EQUILIBRIUM OF X-SECTION FORCES
C
        SUMF=(FAS+FTF+FTW+FTYW+FTEW)-FCEW-FCYW-FCW-FCF
        N=N+1
        IF(ABS(SUMF).LT..1)GO TO 17
        IF(N.LT.2)GO TO 79
        IF(SUMF.LT.0.0)GO TO 70
        IF((SUM-SUMF).LT.0.0.AND.SUM.GT.0.0)GO TO 71
        IF((SUM-SUMF).GT.0.0.AND.SUM.GT.0.0)GO TO 73
        GO TO 74
   70   CONTINUE
        IF((SUM-SUMF).LT.0.0.AND.SUM.LT.0.0)GO TO 75
        IF((SUM-SUMF).GT.0.0.AND.SUM.LT.0.0)GO TO 76
        GO TO 77
   74   CONTINUE
        GO TO 77
   71   CONTINUE
        IF(INCR.LT.0.)GO TO 50
        INCR=-.7*ABS(INCR)
        GO TO 19
   50   CONTINUE
        INCR=.7*ABS(INCR)
        GO TO 19
   73   CONTINUE
        IF(INCR.LT.0.)GO TO 51
        INCR=1.5*ABS(INCR)
        GO TO 19
   51   CONTINUE
        INCR=-1.5*ABS(INCR)
        GO TO 19
   75   CONTINUE
        IF(INCR.LT.0.)GO TO 52
        INCR=1.25*ABS(INCR)
        GO TO 19
   52   CONTINUE
        INCR=-1.25*ABS(INCR)
        GO TO 19
   76   CONTINUE
        IF(INCR.LT.0.)GO TO 53
        INCR=-1.35*ABS(INCR)
        GO TO 19
   53   CONTINUE
        INCR=1.35*ABS(INCR)
        GO TO 19
   77   CONTINUE
        IF(INCR.LT.0.)GO TO 55
        INCR=-.5*ABS(INCR)
        GO TO 19
   55   CONTINUE
        INCR=.5*ABS(INCR)
```

```
      GO TO 19
   79 CONTINUE
      IF(SUMF.LT.0.)GO TO 54
      INCR=ABS(INCR)
      GO TO 19
   54 CONTINUE
      INCR=-1.*ABS(INCR)
   19 CONTINUE
      SUM=SUMF
      Z=Z+INCR
      IF(ICHECK.EQ.2)GO TO 777
      GO TO 763
   17 CONTINUE
      MUAS=FAS*(H+TT+DD-Z)
      MUTF=FTF*(H-Z+(TT/2.))
      MUTW=FTW*((((H-Z-ZZ-ELAST)*2.)/3.)+ZZ+ELAST)
      MUTYW=FTYW*((H-Z-ELAST)/2.+ELAST)
      MUTEW=(FTEW*ELAST*2.)/3.
      IF(ELIST.LE.(H-Z))MUTEW=(FTEW*ELIST*2.)/3.
      MUCEW=(FCEW*ELAST*2.)/3.
      MUCYW=FCYW*((Z-ELAST)/2.+ELAST)
      MUCW=FCW*((((Z-ZZ-ELAST)*2.)/3.)+ZZ+ELAST)
      MUCF=FCF*(Z+TT/2.)
      MULT=(MUTF+MUTYW+MUAS+MUTW+MUCF+MUCYW+MUCW+MUTEW+MUCEW)/12.
      IF(ICHECK.EQ.2)GO TO 778
C
C     AMPS EQUALS MOMENT AT FIRST YIELD OF COMPRESSION FLANGE
C
      AMPS=MULT
      APHI=UNIT
      XMPS=MULT*DIST/(DIST-XOPT)
      WRITE(6,765)XMPS
  765 FORMAT(12X,'ULTIMATE MOMENT BASED ON RECALC. VALUE OF MPS IS ',F8.
     13,'  FT. KIPS')
      WRITE(6,773)XOPT
  773 FORMAT(12X,'OPTIMUM LENGTH FOR LOCAL BUCKLE TO OCCUR IS  ',F7.3,'
     1 INCHES')
      WRITE(6,774)Z
  774 FORMAT(12X,'N.A. LOCATION FOR CALCULATION OF MPS IS ',F6.3,'  INCH
     1ES ABOVE COMPRESSION FLANGE')
      WRITE(6,775)MULT
  775 FORMAT(12X,'CALCULATED VALUE OF MPS IS ',F8.3,'  FT. KIPS',//)
      ICHECK=2
C
C     THIS PART OF THE PROGRAM WILL DEVELOP MOMENT-CURVATURE RELATIONS
C
      ADIST(1)=Z-(H/2.)
      Z=NA-1.5
      IF(AS.LT..0001)Z=H/2.
      PINCR=.00002
      JJ=2
      KJ=2
      SRATIO(1)=0.
      BMTOT(1)=0.
      BPHI(1)=0.
      RCT(1)=0.
      ALOAD(1)=0.
      DELTA(1)=0.
      PHI=UNIT-PINCR
  776 CONTINUE
```

```
      PHI=PHI+PINCR
      UNIT=PHI
      GO TO 777
  778 CONTINUE
      BMTOT(JJ)=MULT
      BPHI(KJ)=PHI
C
C     ADIST EQUALS LOCATION OF N.A. ABOVE CENTER OF STEEL SECTION
C
      ADIST(JJ)=Z-(H/2.)
C
C     DELTA EQUALS CENTERLINE DEFLECTION OF BEAM
C
C
C     XRATIO EQUALS ELASTIC LENGTH OF BEAM
C
      XRATIO=(AMPS*DIST)/BMTOT(JJ)
      IF((BMTOT(JJ)-AMPS).LE..0005)XRATIO=DIST
      SRATIO(JJ)=DIST-XRATIO
      AREA1=XRATIO*.5*BPHI(JJ)
      IF(BPHI(JJ).GT.APHI)AREA1=XRATIO*.5*APHI
      AREA2=(XDIST-DIST)*BPHI(JJ)
      AREA3=(SRATIO(JJ)-SRATIO(JJ-1))*(BPHI(JJ)+BPHI(JJ-1))*.5
      AREA4=AREA4+AREA3
      AREA5=AREA5+AREA3*(XRATIO+SRATIO(JJ-1)+(SRATIO(JJ)/2.))
      ROT(JJ)=2.*(AREA1+AREA2+AREA4)
      DELTA(JJ)=AREA1*XRATIO*2./3.+AREA2*(DIST+.5*(XDIST+DIST))+AREA5
      ALOAD(JJ)=(BMTOT(JJ)*2.*12.)/DIST
      IF(BMTOT(JJ).GT.XMPS)GO TO 779
      IF(ABS(BMTOT(JJ)-XMPS).LE..05)GO TO 780
      JJ=JJ+1
      KJ=KJ+1
      GO TO 776
  779 CONTINUE
      PHI=PHI-PINCR
      PINCR=.1*PINCR
      GO TO 776
  780 CONTINUE
      CALL CALC
      GO TO 11
  909 CONTINUE
      CALL PLOT(0.0,0.0,999)
      STOP
      END
```

```
      SUBROUTINE CALCI
      COMMON ROT(4000)
      COMMON JPLOT,LPAGE,TITLE(20),LPLOT,SECT(10),XMPS,ADIST(4000)
      COMMON A(10),T(10),W(10),E(10),ESH(10),S(10),SSH(10),BMTOT(4000)
      COMMON BPHI(4000),JJ,KJ,ALOAD(4000),DELTA(4000),AIX
      H=T(3)
      TT=T(2)
      DD=T(1)/2.
```

```
      YBAR=(A(1)*(H+2.*TT+DD)+A(2)*(H+1.5*TT)+A(3)*(TT+.5*H)+A(4)*.5*TT)
     1/(A(1)+A(2)+A(3)+A(4))
      WRITE(6,100)YBAR
  100 FORMAT(12X,'CENTROID OF SECTION IS ',F10.3)
      AIX=A(2)*(TT**2/6.+(H+TT+TT/2.-YBAR)**2+(TT/2.-YBAR)**2)+A(3)*(H**
     12/12.+(TT+H/2.-YBAR)**2)+A(1)*((2.*TT+H+DD-YBAR)**2)
      RETURN
      END




      SUBROUTINE CALC
      COMMON ROT(4000)
      COMMON JPLOT,LPAGE,TITLE(20),LPLOT,SECT(10),XMPS,ADIST(4000)
      COMMON A(10),T(10),W(10),E(10),ESH(10),S(10),SSH(10),BMTOT(4000)
      COMMON BPHI(4000),JJ,KJ,ALOAD(4000),DELTA(4000),AIX
      WRITE(6,20)
   20 FORMAT(12X,'MOMENT CURVATURE RELATIONSHIPS - COMPOSITE BEAMS -'
     2' NEGATIVE BENDING' //)
      WRITE(6,25)
   25 FORMAT (           '     BEAM DATA     (REBAR,FLANGE,WEB,FLANGE,AND COVERPL
     2 COVERPLATE RESPECTIVELY)'//          '     AREA   THICKNESS    WID
     3TH,        E           ESH     SIGMA Y   SIGMA SH',/)
      L=JJ-10
      DO 100 K=1,5
      WRITE(6,24)A(K),T(K),W(K),E(K),ESH(K),S(K),SSH(K)
   24 FORMAT(1X,3F10.3,2F12.1,2F10.6    )
  100 CONTINUE
      WRITE(6,6246)AIX
 6246 FORMAT(12X,'MOMENT OF INERTIA OF SECTION IS ',F8.3,' INCHES**4',/)
       WRITE(6,6245)
 6245 FORMAT(  'CHECK',///)
      DO 200 I=L,JJ
      WRITE(6,300)BMTOT(I),BPHI(I),ADIST(I),ALOAD(I),DELTA(I),ROT(I)
  300 FORMAT(12X,F10.3,F10.6,F10.3,F8.3,F10.6,2X,F10.6)
  200 CONTINUE
       CALL GRAPH
      RETURN
      END




      SUBROUTINE GRAPH
      COMMON ROT(4000)
      COMMON JPLOT,LPAGE,TITLE(20),LPLOT,SECT(10),XMPS,ADIST(4000)
      COMMON A(10),T(10),W(10),E(10),ESH(10),S(10),SSH(10),BMTOT(4000)
      COMMON BPHI(4000),JJ,KJ,ALOAD(4000),DELTA(4000),AIX
      IF(A(1).LT..0001.AND.JPLOT.GT.1)CALL PLOT(12.,-19.,-3)
      IF(A(1).LT..0001)JPLOT=JPLOT+1
      NNKK=0
```

```
      BPHI(KJ+1)=0.0
      ALOAD(JJ+1)=0.
      RCT(JJ+1)=0.
      DELTA(JJ+1)=0.
      ADIST(JJ+1)=0.
      BMTOT(JJ+1)=0.0
      IF(LPLOT.EQ.3)GO TO 31
      IF(LPLOT.EQ.4)GO TO 32
      IF(LPLOT.EQ.5)GO TO 33
      IF(LPLOT.EQ.6)GO TO 36
      IF(LPLOT.EQ.7)GO TO 37
      IF(LPLOT.EQ.8)GO TO 38
      IF(LPLOT.EQ.9)GO TO 39
      IF(LPLOT.EQ.10)GO TO 40
      IF(LPLOT.EQ.11)GO TO 41
      IF(LPLOT.EQ.12)GO TO 42
      BPHI(KJ+2)=.004
      BMTOT(JJ+2)=60.
      DELTA(JJ+2)=1.
      ALOAD(JJ+2)=30.
      ADIST(JJ+2)=1.
      RCT(JJ+2)=.03
      GO TO 34
   31 CONTINUE
      DELTA(JJ+2)=1.
      ALOAD(JJ+2)=15.
      ADIST(JJ+2)=1.
      RCT(JJ+2)=.03
      BMTOT(JJ+2)=25.
      BPHI(KJ+2)=.0001
      GO TO 34
   32 CONTINUE
      BMTOT(JJ+2)=50.
      BPHI(KJ+2)=.004
      DELTA(JJ+2)=1.
      ALOAD(JJ+2)=30.
      ADIST(JJ+2)=1.
      RCT(JJ+2)=.03
      GO TO 34
   33 CONTINUE
      BMTOT(JJ+2)=25.
      BPHI(KJ+2)=.0007
      DELTA(JJ+2)=1.
      ALOAD(JJ+2)=15.
      ADIST(JJ+2)=1.
      RCT(JJ+2)=.03
      GO TO 34
   36 CONTINUE
      BMTOT(JJ+2)=25.
      BPHI(KJ+2)=.0003
      DELTA(JJ+2)=.25
      ALOAD(JJ+2)=15.
      ADIST(JJ+2)=1.
      RCT(JJ+2)=.005
      GO TO 34
   37 CONTINUE
      BPHI(KJ+2)=.002
      BMTOT(JJ+2)=60.
      DELTA(JJ+2)=1.
      ALOAD(JJ+2)=30.
```

```
      ADIST(JJ+2)=1.
      ROT(JJ+2)=.03
      GO TO 34
   38 CONTINUE
      BMTOT(JJ+2)=60.
      BPHI(KJ+2)=.0015
      DELTA(JJ+2)=1.
      ALOAD(JJ+2)=30.
      ADIST(JJ+2)=1.
      ROT(JJ+2)=.03
      GO TO 34
   39 CONTINUE
      BMTOT(JJ+2)=60.
      BPHI(KJ+2)=.001
      DELTA(JJ+2)=1.
      ALOAD(JJ+2)=30.
      ADIST(JJ+2)=1.
      ROT(JJ+2)=.03
      GO TO 34
   40 CONTINUE
      BMTOT(JJ+2)=50.
      BPHI(KJ+2)=.002
      DELTA(JJ+2)=1.
      ALOAD(JJ+2)=30.
      ADIST(JJ+2)=1.
      ROT(JJ+2)=.03
      GO TO 34
   41 CONTINUE
      BMTOT(JJ+2)=50.
      BPHI(KJ+2)=.001
      DELTA(JJ+2)=1.
      ALOAD(JJ+2)=30.
      ADIST(JJ+2)=1.
      ROT(JJ+2)=.03
       GO TO 34
   42 CONTINUE
      BMTOT(JJ+2)=50.
      BPHI(KJ+2)=.0005
      DELTA(JJ+2)=1.
      ALOAD(JJ+2)=30.
      ADIST(JJ+2)=1.
      ROT(JJ+2)=.03
   34 CONTINUE
      IF(A(1).GT..0001.AND.NNKK.EQ.0)GO TO 25
      IF(A(1).GT..0001.AND.NNKK.EQ.1)GO TO 101
      IF(A(1).GT..0001.AND.NNKK.EQ.2)GO TO 102
      IF(A(1).GT..0001.AND.NNKK.EQ.3)GO TO 103
      CALL PLOT(0.0,0.0,3)
      CALL PLOT(0.0,8.5,2)
      CALL PLOT(11.0,8.5,2)
      CALL PLOT(11.0,0.0,2)
      CALL PLOT(0.0,0.0,2)
      CALL PLOT(1.25,1.25,3)
      CALL PLOT(1.25,7.45,2)
      CALL PLOT(9.75,7.45,2)
      CALL PLOT(9.75,1.25,2)
      CALL PLOT(1.25,1.25,2)
      CALL SYMBOL(1.0,9.0,0.1,TITLE,0.0,80)
      CALL SYMBOL(8.0,2.7,0.15,SECT,0.0,8)
      CALL PLOT(2.0,2.0,-3)
```

```
      IF(NNKK.EQ.1)GO TO 100
      IF(NNKK.EQ.3)GO TO 105
      CALL AXIS(0.0,0.0,14HMOMENT-FT.KIPS,14,5.0,90.0,BMTOT(JJ+1),BMTOT(
     1JJ+2),20.0)
      IF(NNKK.EQ.2)GO TO 104
      CALL AXIS(0.0,0.,22HCURVATURE-RADIANS/INCH,-22,7.0,0.0,BPHI(KJ+1),
     1BPHI(KJ+2),20.0)
   25 CONTINUE
      IF(A(1).GT..0001)CALL PLOT(-14.,-17.,-3)
      CALL LINE(BPHI,BMTOT,JJ,1,0,0)
      IF(A(1).LT..0001)CALL PLOT(-2.,15.,-3)
      NNKK=1
      GO TO 34
  100 CONTINUE
      CALL AXIS(0.,0.,17HAPPLIED LOAD-KIPS,17,5.,90.0,ALOAD(JJ+1),ALOAD(
     1JJ+2),20.0)
      CALL AXIS(0.,0.,29HCENTRE LINE DEFLECTION-INCHES,-29,7.,0.,DELTA(J
     1J+1),DELTA(JJ+2),20.0)
  101 CONTINUE
      IF(A(1).GT..0001)CALL PLOT(0.,17.,-3)
      CALL LINE(DELTA,ALOAD,JJ,1,0,0)
      IF(A(1).LT..0001)CALL PLOT(12.,-19.,-3)
      NNKK=2
      GO TO 34
  104 CONTINUE
      CALL AXIS(0.,0.,16HROTATION-RADIANS,-16,7.,0.,ROT(JJ+1),ROT(JJ+2),
     120.)
  102 CONTINUE
      IF(A(1).GT..0001)CALL PLOT(14.,-17.,-3)
      CALL LINE(ROT,BMTOT,JJ,1,0,0)
      IF(A(1).LT..0001)CALL PLOT(-2.,15.,-3)
      NNKK=3
      GO TO 34
  105 CONTINUE
      CALL AXIS(0.,0.,14HMOMENT-FT.KIPS,-14,5.,0.,BMTOT(JJ+1),BMTOT(JJ+2
     1),20.)
      CALL AXIS(0.,0.,28HNEUTRAL AXIS LOCATION-INCHES,28,5.,90.,ADIST(JJ
     1+1),ADIST(JJ+2),20.)
  103 CONTINUE
      IF(A(1).GT..0001)CALL PLOT(0.,17.,-3)
      IF(A(1).GT..0001)CALL LINE(BMTOT,ADIST,JJ,1,0,0)
      DO 14 I=1,4000
      BMTOT(I)=0.
      BPHI(I)=0.
      ALOAD(I)=0.
      DELTA(I)=0.
      ROT(I)=0.
      ADIST(I)=0.
   14 CONTINUE
      RETURN
      END
```